

# JGR Biogeosciences

## RESEARCH ARTICLE

10.1029/2021JG006592

### Key Points:

- The 2017 Atmospheric River event delivered historic rain amounts and increased flooding in marshes of San Francisco Bay, California, USA
- The marshes located within the riverine geomorphic setting were more influenced by storm flooding and had greater elevation response
- Interactions among marshes and storms, flooding, and accretion is critical in understanding how climate change will impact estuaries

### Supporting Information:

Supporting Information may be found in the online version of this article.

### Correspondence to:

K. Thorne,  
[ktthorne@usgs.gov](mailto:ktthorne@usgs.gov)

### Citation:

Thorne, K., Jones, S., Freeman, C., Buffington, K., Janousek, C., & Guntenspergen, G. (2022). Atmospheric river storm flooding influences tidal marsh elevation building processes. *Journal of Geophysical Research: Biogeosciences*, 127, e2021JG006592. <https://doi.org/10.1029/2021JG006592>

Received 20 AUG 2021

Accepted 2 MAR 2022

### Author Contributions:

**Conceptualization:** Karen Thorne, Christopher Janousek

**Data curation:** Scott Jones, Chase Freeman, Kevin Buffington

**Formal analysis:** Scott Jones, Chase Freeman, Kevin Buffington







**Funding acquisition:** Karen Thorne, Christopher Janousek, Glenn Guntenspergen

**Investigation:** Chase Freeman, Kevin Buffington, Christopher Janousek

**Methodology:** Karen Thorne, Chase Freeman, Christopher Janousek, Glenn Guntenspergen

© 2022 American Geophysical Union. All Rights Reserved. This article has been contributed to by U.S. Government employees and their work is in the public domain in the USA.

## Atmospheric River Storm Flooding Influences Tidal Marsh Elevation Building Processes

Karen Thorne<sup>1</sup> , Scott Jones<sup>1</sup> , Chase Freeman<sup>1</sup> , Kevin Buffington<sup>1</sup> , Christopher Janousek<sup>2</sup> , and Glenn Guntenspergen<sup>3</sup> 

<sup>1</sup>Western Ecological Research Center, U.S. Geological Survey, Davis, CA, USA, <sup>2</sup>Department of Fisheries, Wildlife and Conservation Sciences, Oregon State University, Corvallis, OR, USA, <sup>3</sup>Eastern Ecological Science Center, U.S. Geological Survey, Laurel, MD, USA

**Abstract** Disturbances are a key component of ecological processes in coastal ecosystems. Investigating factors that affect tidal marsh accretion and elevation change is important, largely due to accelerating sea-level rise and the ecological and economic value of wetlands. Sediment accumulation rates, elevation change, and flooding were examined at five marshes along a riverine-tidal gradient in the northern San Francisco Bay-Delta, California, USA during an Atmospheric River storm event in 2017 using Surface Elevation Tables (SETs), feldspar marker horizons (MH), and continuous water-level sensors. Our results showed that localized marsh flooding increased during the storm event, but not evenly across sites. Marsh surface elevation increased the most at the tidal freshwater marsh site in response to the storms, with an average surface elevation gain of  $45.6 \pm 13.1$  mm, and the least at a tidal saline marsh with an average surface elevation gain of  $4.0 \pm 1.2$  mm. A marsh located on the large embayment did not exhibit an immediate response to the storm but had a surface elevation gain of  $21.5 \pm 13.7$  mm 6 months after the storm. During the storm period, marsh distance to the bay was the strongest predictor of elevation change, followed by SET-MH elevations. Conversely, during non-storm periods, SET-MH elevation was a relatively strong predictor of elevation change. Atmospheric Rivers appear to be a major factor affecting short-term spatial and temporal variability in flooding and sedimentation rates in tidal marsh systems. Incorporating information about storms into monitoring could increase our understanding of how episodic storms can impact marshes.

**Plain Language Summary** Coastal tidal marshes occur between land and sea and get flooded daily by tides and river flows. Ocean and river waters can deliver sediment to marshes to build their elevations to prevent drowning. Atmospheric Rivers are extreme precipitation events in which the amount of water typically delivered in a year happens in just a few days. These types of storms can increase flood waters and sediment delivery to marshes. In 2017 Atmospheric River storms increased the flooding in marshes of San Francisco Bay-Delta, California, USA when compared with non-storm periods. This flooding increased elevation at the marshes that were more closely associated with a riverine setting. This information is important in understanding marsh processes and how it related to storms, which are projected to change in frequency and intensity under a warming climate.

## 1. Introduction

Natural storm disturbances span a large range of sizes, intensities, and frequencies, which can shape landforms and influence ecosystems; the importance of landscape disturbance regimes is gaining recognition given changing weather patterns with climate change (Turner, 2010). Coastal storms can produce significant amounts of precipitation and increase ocean water levels and wave heights. These large infrequent disturbances (Dale et al., 1998; Romme et al., 1998; Turner, 2010) can include tropical cyclones (i.e., hurricanes) and other low-pressure high precipitation events (i.e., Atmospheric Rivers). Episodic storms can amplify ocean flooding in coastal areas when heavy precipitation, river discharge, and storm surges co-occur, impacting infrastructure and populations especially in developed coastlines (Wahl et al., 2015). Understanding flooding risk is important with over 630 million people worldwide living within the coastal zone and with future population growth projected to increase to over 1 billion people by mid-century (Merkens et al., 2016). Currently, about 40% of the USA population resides in coastal areas (NOAA, 2013).

**Project Administration:** Karen Thorne, Christopher Janousek, Glenn Guntenspergen  
**Resources:** Glenn Guntenspergen  
**Supervision:** Karen Thorne, Glenn Guntenspergen  
**Visualization:** Karen Thorne  
**Writing – original draft:** Karen Thorne, Chase Freeman, Kevin Buffington  
**Writing – review & editing:** Karen Thorne, Scott Jones, Chase Freeman, Kevin Buffington, Christopher Janousek, Glenn Guntenspergen

When episodic storm flooding is paired with predicted sea-level rise rates, negative impacts to human populations and property could occur due to flood exposure (Alizad et al., 2018; Barnard et al., 2019; Carvajal et al., 2021), with uncertain consequences to ecosystems. However, coastal ecosystems can provide protection and barriers from flooding (Temmerman et al., 2013). Tidal marshes serve as coastal flood protection by reducing wave impacts and absorbing storm surges with a suggested economic value over \$190,000 USD/ha (Vázquez-González et al., 2019) for flood protection. Flooding from warmer ocean conditions during El Niño storm events can increase normal flooding time and depth in tidal marshes, illustrating their flooding tolerance (Goodman et al., 2018; Harvey et al., 2020). Dynamic water levels from episodic storms drive coastal flooding (Wahl et al., 2015) that can cause beach and dune erosion (Castelle et al., 2015) and cliff retreat (Moore & Griggs, 2002).

Localized and temporary disturbances from storms and flooding on marsh vegetation can trigger permanent loss of elevation and vegetation (Kirwan et al., 2008). Extreme storms could impact marsh plants by increased inundation and wave energy damaging standing biomass and can become stressed by prolonged flooding. Marsh vegetation dieback has been well documented following hurricane storm surges (Hauser et al., 2015; Morton & Barras, 2011; Ramsey et al., 2014; Yeates et al., 2020), but is less documented for storms that create chronic prolonged flood events but don't have associated severe winds and waves like hurricanes (Stagg et al., 2021). In experimental settings, marsh plants can tolerate some smothering by applied sediments (Payne, 2021), and prolonged freshwater flooding (Buffington et al., 2020; Sharpe & Baldwin, 2012). Prolonged storm flooding can impact marsh plants as many species have very narrow flooding tolerances (Janousek et al., 2016, 2019; Kirwan & Guntenspergen, 2015); however, if drainage of storm waters occurs plants can recover from the flooding. Interestingly, if the marsh is flushed by fresh storm waters, it may increase plant productivity by reducing saline soils (Cahoon, 2006).

Anomalous flooding events in marshes can also impact resident wildlife by increasing predation (Thorne et al., 2019), displacing individuals during high water events (Smith et al., 2014), or reducing fecundity (Correll et al., 2017; Van De Pol et al., 2010). Van De Pol et al. (2010) suggests that unpredictable extreme flood events in lower elevation habitats may function as ecological traps for tidal marsh birds and decrease avian biodiversity. However, extended flooding in tidal marshes can also provide food resources for aquatic animals. For example, fish and crustacean species can use flooded tidal marshes as nurseries and foraging areas (Larkin et al., 2008; Peterson & Turner, 1994).

Atmospheric Rivers (AR) are warm, low-level jet stream storms with strong seasonality that transport condensed water vapor inland, resulting in heavy precipitation over several days (American Meteorological Society, 2018; Lavers & Villarini, 2015; Zhu & Newell, 1998). During these land-falling storm events, heavy rains can result in flooding, mud slides, strong winds and other hazards (A. B. Smith, 2020). For example, a hazardous AR in February 2017 led to the weakening of the Oroville Dam in northern California, USA and mass evacuations of people in nearby cities (M. Taylor, 2017). ARs have also been attributed to the 10 largest winter flood events between 1970 and 2010 in the United Kingdom (Lavers et al., 2011). However, many ARs do not result in hazardous conditions and are beneficial by replenishing freshwater in reservoirs and increasing snowpack, providing drought relief (Dettinger, 2013). ARs can contribute 30%–50% of annual precipitation along the Pacific Coast of North America over just a few days (Dettinger, 2013), which is particularly important within the Mediterranean climate zone where annual precipitation occurs during a narrow winter time period (Dettinger, 2011). ARs have also been documented to cause 20%–30% of all precipitation in parts of Europe (Lavers & Villarini, 2015). Coastal ecosystem impacts by AR events are rarely documented in the literature due to their stochastic nature but could have significant ecological impacts over the near and long-term.

Tidal marshes are coastal ecosystems that are governed by physical and biological processes creating a system that is in a dynamic equilibrium with water levels. To prevent long-term submergence of tidal marshes with sea-level rise, accretion processes or upland transgression needs to occur (Langston et al., 2021; Schieder et al., 2018; Thorne et al., 2018). Accretion builds tidal marsh platform elevations and is defined as the vertical growth of the soils by organic and mineral sediments as well as autochthonous plant growth (Nyman et al., 2006). Inorganic sediment contributions to tidal marshes can come from either marine or riverine sources (Cahoon et al., 1996). Accretion is one of the key factors in determining if a tidal marsh can build elevation quickly enough to keep pace with sea-level rise rates; if there is an insufficient amount of material, then submergence of the wetland will occur (Alizad et al., 2016; Craft et al., 2009; Kirwan et al., 2010; Schile et al., 2014; Thorne et al., 2018). Understanding the links between marsh flooding and accretion is important for assessing their long-term ecological

response to varying flooding, particularly since precipitation is predicted to become flashier and more volatile in many regions of the world (Polade et al., 2017). Episodic pulses of sediment accumulation during storms may be an important mechanism for tidal marshes to keep pace with sea-level rise, especially to compensate for periods of sediment deficits or when rates of accumulation are less than the rate of relative sea-level rise (McKee & Cherry, 2009).

Large infrequent storm events are geomorphologically and ecologically important agents of change in tidal marshes, potentially altering surface elevation trajectories because of sediment deposition or erosion (Cahoon, 2006; Cahoon et al., 1996; Yeates et al., 2020). Several studies in other regions have shown long term trends of storm flooding linked to tidal marsh accretion (Cahoon et al., 1996; Schuerch et al., 2013), but little has been documented about large infrequent storm disturbances and accretion response for the Pacific Coast of North America. Some studies have evaluated the impact of major coastal storms on wetland soil elevations, with most of those studies examining the impacts from hurricanes (Cahoon, 2006; Feher et al., 2020; Guntenspergen et al., 1995; McKee & Cherry, 2009; Turner et al., 2006). For example, a tidal marsh in Germany had increased accretion rates that coincided with increased storm frequency, especially in the lower tidal marsh zone (Schuerch et al., 2012). Storms can also increase erosion and therefore influence deposition in adjacent tidal marshes, contributing to elevation building processes. Using a modeling approach, Schuerch et al. (2013) showed that an increase in storm frequency increased the ability of a marsh on the German island of Sylt to accrete up to 3 mm yr<sup>-1</sup>, given the availability of erodible fine-grained material nearby.

The morphodynamics of tidal marshes along riverine deltas and estuaries are also associated with landform and geomorphic properties. River flooding is another important source of sediments to tidal marshes in estuaries (Day et al., 1995). River floods can transport very high sediment loads after storm events and can drive the geomorphic evolution of the coast, and a few studies have used surface elevation tables (SETs) to track changes in elevation and accretion in coastal wetlands due to river flooding (Cahoon et al., 1996; Day et al., 1995; Hensel et al., 1998). Day et al. (1995) and Hensel et al. (1998) found that the highest sedimentation rates in the Rhone River delta were measured at riverine sites. Accretion in a *Spartina foliosa* low marsh site in the Tijuana Estuary, California, was related almost entirely to episodic storm-induced river flows (Cahoon et al., 1996).

Research on the impacts of ARs across an estuarine gradient is lacking and the role of these large infrequent disturbances in regulating the function, structure, and accretion of tidal marshes is not well documented throughout the world. ARs that made landfall along the California (USA) coastline during the winter season of November 2016 to February 2017 ranged in strength from Moderate (AR Cat 2) to Exceptional (AR Cat 5) and resulted in unprecedented precipitation amounts (Ralph et al., 2019). The water year (begins every October 1st) 2016–2017 was the second wettest year in a 122 years of record for this region (Wang et al., 2017), with precipitation amounts exceeding 100 cm in January and February of 2017 (Wen et al., 2018). Here, our objective was to evaluate the influence of the 2016–2017 AR on marsh accretion and elevation change and investigate the spatial variability in response along an estuarine gradient in the San Francisco Bay-Delta estuary, California (USA). We hypothesized that increased flooding from ARs would increase accretion rates and elevation change of the marsh which will vary across the estuary. We examined what factors may have influenced marsh accretion and elevation change in response to ARs across different scales. Landscape factors we assessed included the distances from water and sediment sources and size of those features (local channel, larger watershed, bay) and local site characteristics (elevation, flooding amount).

## 2. Methods

### 2.1. Study Sites

California's San Francisco Bay-Delta estuary is one of the largest estuaries on the Pacific Coast of North America and is home to over 7 million people, with an extensive agriculture industry and diverse economy (United States Census Bureau, 2019). Here, the Sacramento River and the San Joaquin River join at the Delta portion of San Francisco Bay with river flows moving through Suisun Bay, San Pablo Bay, and then, into central San Francisco Bay with an entrance to the open ocean through the Golden Gate. These major rivers and smaller tributaries in Northern California deliver much of the freshwater and sediment to the estuary (Cloern & Jassby, 2012), with the active tributaries accounting for only 5% of the total watershed area but contributing 61% of the suspended sediment (McKee et al., 2013). This region has a Mediterranean climate with warm dry summers and mild wet

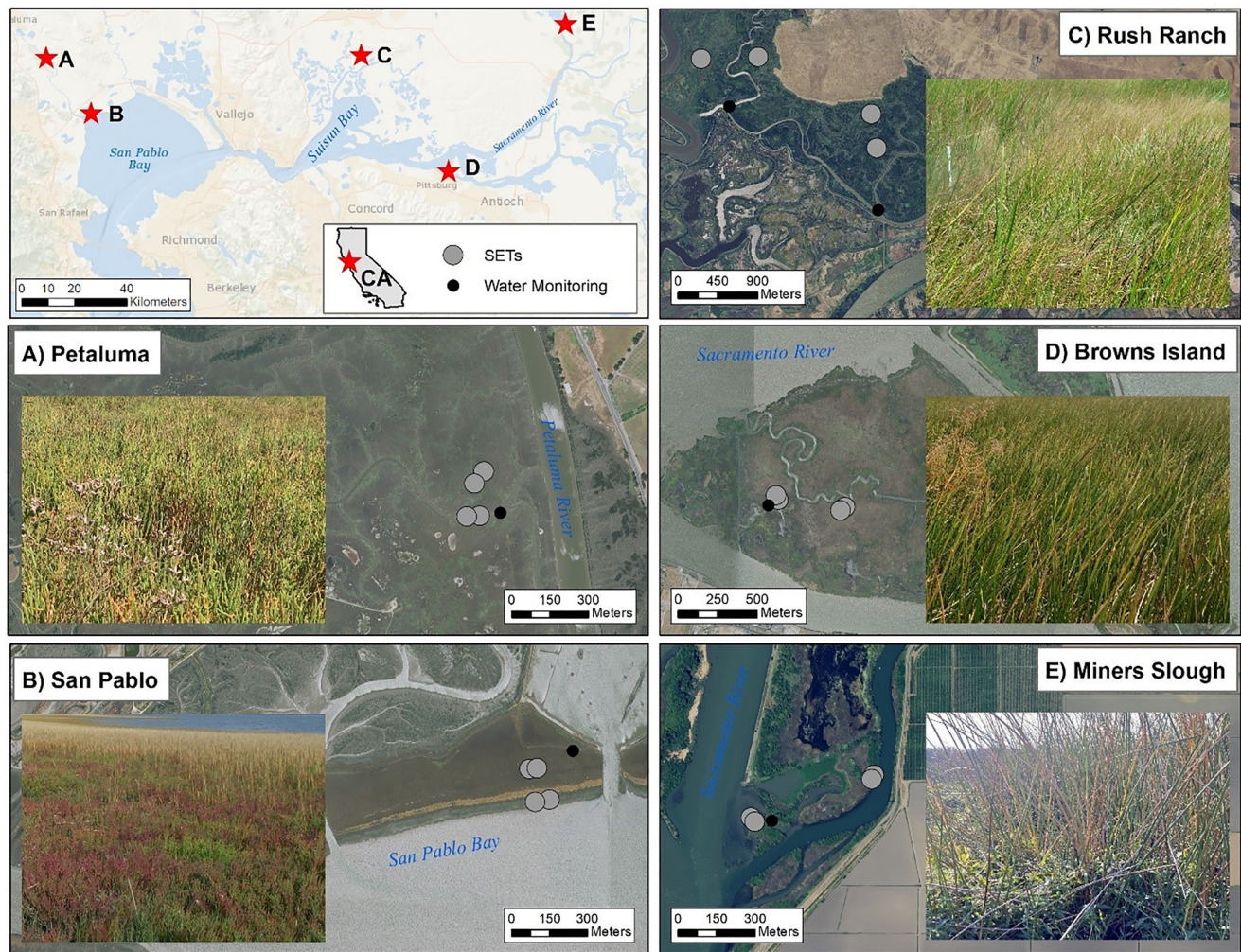


**Figure 1.** Study sites were located along a tidal and salinity gradient in the San Francisco Bay-Delta, CA. Each marsh location is in a different geomorphic setting in the estuary and has a variety of dominant vegetation. Gray circles represent Surface Elevation Table (SET)-marker horizon (MH) locations and black circles are water monitoring locations for each marsh site.

winters with highest river discharge occurring during winter and spring months. The estuary has a mixed semi-diurnal tidal regime with water levels influenced by tides, fresh-water inflow, and lower frequency ocean fluctuations driven by multi-annual climate variability such as the El Niño Southern Oscillation. Study sites spanned a tidal and salinity gradient in the northern portion of the estuary, offering an opportunity to quantify the effects of an infrequent disturbance storm event on marsh processes at the estuary scale (Figure 1).

We examined five tidal marsh sites along an estuarine gradient from riverine dominated to ocean dominated with a range of salinities and tides (Figure 1 and Table 1). San Pablo marsh (hereafter San Pablo) is located within the San Pablo Bay National Wildlife Refuge, which is directly adjacent to San Pablo Bay and is predominately dominated by ocean tides with occasional fresh-water delivery from creek and riverine inflows. Petaluma marsh (hereafter Petaluma) is a large tidal marsh dominated by oceanic drivers, with infrequent pulses of fresh-water and a high elevation platform located along the Petaluma River north of San Pablo Bay. Rush Ranch Open Space marsh (hereafter Rush Ranch) is in northern Suisun Bay and is an extensive oligohaline to mesohaline marsh complex. It is influenced by tides, Delta river flows, and local creeks. Browns Island marsh (hereafter Browns Island), a preserve of the East Bay Regional Park District, is an oligohaline riverine marsh located at the western side of the Sacramento-San Joaquin River Delta and is influenced by tides and Delta river flows. Miner Slough Wildlife Area (hereafter Miner Slough) is a tidal fresh-water riverine marsh located next to the Sacramento Deep Water Channel in the northern Delta and is influenced primarily by river flows.

**Table 1**

*Geomorphic Setting Within the Estuary for Each Marsh Study Site Including Marsh Platform Elevation, Tide, Salinity, and Watershed Characteristics and Location Relative to Local Watershed*

Site (abbreviation)	Geomorphic setting									
	Elevation (NAVD88, m)		Site tide range (MHHW-MLLW; m)	Salinity ppt range (mean)	Distance to San Pablo bay edge (kilometers)	Nearest channel (m)		Watershed		
	Range	Median				Distance to	Cross-sectional size of	Name	Size (sq miles)	Length (miles)
Petaluma marsh (Petaluma)	0.02–2.56	2.14	1.94*	0–35 (15)	12	74	22	Petaluma River	146	19
San Pablo NWR marsh (San Pablo) <sup>a</sup>	0.09–2.62	1.84	1.87**	13–35 (19)	0	154 <sup>b</sup>	NA	Petaluma River	146	19
Rush Ranch	0.27–2.50	1.97	1.66***	1–10 (3)	32 (20 <sup>c</sup> )	241	43	Sacramento & San Joaquin Rivers	43,100	760
Browns Island	0.42–2.58	1.71	1.35***	1–9 (2)	33	51	20	Sacramento & San Joaquin Rivers	43,100	760
Miner Slough	0.59–2.28	1.43	1.21***	0–1 (0)	66	15	144	Sacramento River	27,500	400

Note. \*From NOAA gauge; \*\*Estimated from VDATUM; \*\*\*Empirically measured.

<sup>a</sup>San Pablo is on the bay edge and has Petaluma River watershed on the west side. <sup>b</sup>distance to Bay Edge. <sup>c</sup>Measurement to center of Sacramento River directly south of Rush Ranch.

Watershed size, which is governed by study site location, is an important element of riverine versus coastal influence (Table 1). San Pablo is located along the edge of San Pablo Bay and is mainly bay/tidally influenced, but local tributaries include Sonoma Creek watershed on its eastern side and the Petaluma River watershed on its western side. Petaluma is within the Petaluma River watershed that is small when compared with the Sacramento and San Joaquin Rivers. Rush Ranch is within the Sacramento and San Joaquin river watersheds; however, it is located north of the main river channel within Suisun Bay and therefore does not get the direct effects of the riverine flows. Browns Island and Miner Slough are located next to major channels of the Sacramento and San Joaquin river watershed and are therefore strongly influenced by these large rivers.

## 2.2. Geomorphic and Landscape Setting

Along the ocean-riverine forcing gradient are additional landscape drivers that influence marsh processes, including distance to San Pablo Bay edge (proxy for salinity and tidal/riverine forcing), distance to nearest channel, cross-sectional size of that channel, tide range, and marsh elevations. To characterize the hydrologic and geomorphic setting of each site, we deployed automated environmental sensors and conducted spatial analysis. Distance to San Pablo Bay edge, nearest channel, and cross-sectional size of that channel were measured in ArcGIS 10.7 (Environmental Systems Research Institute Inc.) using the distance tool. Distance to San Pablo Bay edge was measured as the length from the confluence of the bay and the river (Petaluma or Sacramento) along the curvature of the river to the study site, whereas distance to channel was measured as a linear line to the channel edge.

To further characterize the tidal marsh study sites, we assessed the overall elevation of the marsh platform using published vegetation-corrected lidar (Buffington et al., 2016). For San Pablo and Petaluma marsh, we used a published digital elevation model (Buffington & Thorne, 2019), and for Rush Ranch and Browns Island, we used data from Buffington et al. (2019) to determine the marsh platform elevations. For Miner Slough, we determined wetland surface elevations with a Leica survey-grade GNSS rover (Viva GS15 and RX1250X models) using GPS real-time kinematic (RTK) corrections (manufacturer-published horizontal precision  $\pm 1$  cm and vertical precision  $\pm 4$  cm; Leica Geosystems Inc., Norcross, GA). Data corrections were streamed to the rover via an internet connection to GNSS base-station networks (Leica Smartnet, [www.smartnetna.com](http://www.smartnetna.com)), with the average measured vertical error being within the  $\pm 2$  cm error of the RTK at local benchmarks. Ellipsoid heights of the wetland surface were processed with Leica Geomatics software to determine orthometric heights using the North American Vertical Datum of 1988 (NAVD88) and the geoid 12A model. We used our RTK GPS surveyed elevations in conjunction with remotely sensed light detection and ranging (lidar) data and normalized difference vegetation index (NDVI) data to generate high-resolution (1 m) digital elevation models (DEMs) of wetland surface

**Table 2**

Within Marsh Biogeomorphic Characterization for Each Surface Elevation Table (SET)-Marker Horizon (MH) Location Including Dominant Plant Species, Elevations, and Nearest Channel

Site (abbreviation)	Surface elevation-MH location (UTM10 N)		Dominant plant species	Elevation (m, NAVD88)	Elevation (m above MSL)	Z*
	Northing	Easting				
Petaluma marsh (Petaluma)						
SET1	4227122	539405	<i>Salicornia pacifica</i>	1.97	0.89	0.98
SET2	4227168	539442	<i>S. pacifica</i>	1.93	0.85	0.94
SET3	4226991	539377	<i>S. pacifica</i>	2.02	0.94	1.03
SET4	4226996	539425	<i>S. pacifica</i>	2.01	0.93	1.02
San Pablo NWR marsh (San Pablo)						
SET1	4218709	546078	<i>Spartina foliosa</i>	1.28	0.20	0.23
SET2	4218717	546133	<i>S. foliosa</i>	1.28	0.20	0.24
SET3	4218836	546056	<i>S. pacifica</i>	1.99	0.91	1.08
SET4	4218844	546083	<i>S. pacifica</i>	1.98	0.9	1.08
Rush Ranch NERR (Rush Ranch)						
SET1	4227786	586310	<i>Juncus balticus</i> , <i>Distichlis spicata</i>	2.02	0.95	1.08
SET2	4227407	586368	<i>J. balticus</i> , <i>Schoenoplectus americanus</i>	1.97	0.90	1.02
SET3	4228436	585022	<i>S. pacifica</i> , <i>D. spicata</i>	2.02	0.95	1.08
SET4	4228411	584367	<i>D. spicata</i> , <i>S. pacifica</i>	2.01	0.94	1.07
Browns Island						
SET1	4210677	599080	<i>Typha</i> spp., <i>Schoenoplectus acutus</i>	1.30	0.18	0.26
SET2	4210706	599067	<i>S. americanus</i> , <i>S. acutus</i>	1.41	0.29	0.41
SET3	4210630	599504	<i>S. americanus</i>	1.77	0.65	0.91
SET4	4210608	599475	<i>S. americanus</i>	1.81	0.69	0.97
Miner Slough						
SET1	4232807	616720	<i>S. californicus</i> , <i>S. acutus</i>	1.53	0.31	0.53
SET2	4232791	616710	<i>S. californicus</i> , <i>S. acutus</i>	1.34	0.12	0.20
SET3	4232640	616239	<i>Cornus sericea</i> , <i>Typha</i> spp., <i>S. acutus</i>	1.74	0.52	0.88
SET4	4232636	616238	<i>C. sericea</i> , <i>Typha</i> spp., <i>S. acutus</i>	1.63	0.42	0.70

Note. \*From NOAA gauge; \*\*Estimated from VDATUM; \*\*\*Empirically measured. Nyman et al., 2006.

topography using the LEAN method (see Buffington et al., 2016) to correct for positive bias due to vegetation cover. We obtained lidar derived DEMs from the NOAA Digital Coastal Data Access Viewer (NOAA, 2018) and multispectral airborne imagery data from the National Agriculture Imagery Program (U.S. Department of Agriculture Farm Service Agency). From the National Agriculture Imagery Program imagery, we calculated NDVI =  $([NIR\ Red]/[NIR + Red])$ , where Red included wavelengths of 608–662 nm and NIR included wavelengths of 833–887 nm. Next, we calculated lidar error by subtracting the lidar DEM from the RTK-GPS data and then used a multivariate linear regression approach to model the relationship between lidar error. For each site, we filtered DEMs to include only elevations between the mean lower low water (MLLW) datum and highest observed tide for each specific site.

### 2.3. Marsh Accretion and Elevation Change

We installed deep rod Surface Elevation Table (SET) and feldspar marker horizon (MH) plots (Figure 1 and Table 2) to quantify the relative contributions of surface and subsurface processes to vertical accretion and elevation change (Cahoon & Turner 1989; Cahoon et al., 2002) in each of the five study marshes. The SET-MHs were installed in San Pablo during 2013, whereas SET-MH installation at the other four sites occurred in 2016. A

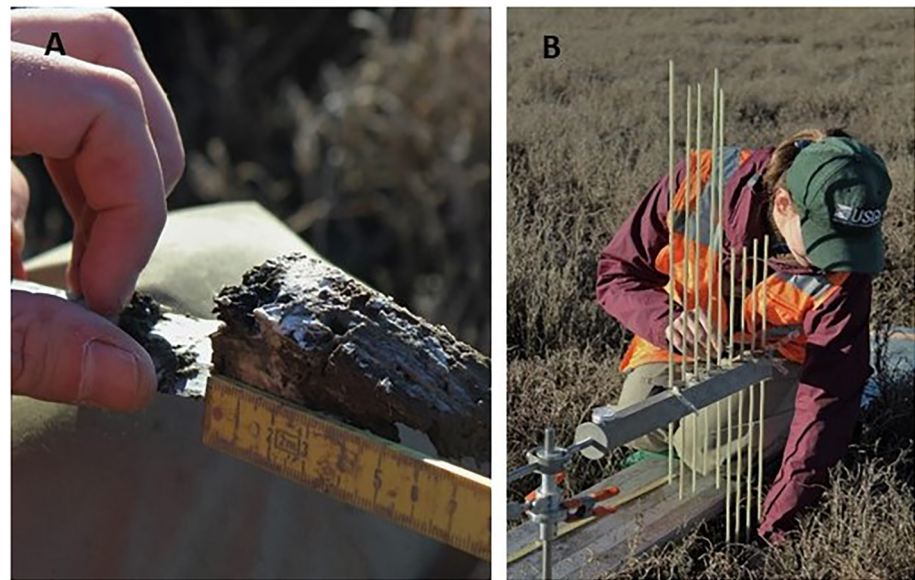


**Figure 2.** (a) Reading marker horizon (MH) feldspar layer provides an estimate of how much material has been deposited on the marsh surface to estimate accretion, (b) Surface Elevation Tables (SETs) provide information on total elevation change of a marsh surface and incorporate below-ground and surface processes.

summary of the SET-MH protocol was published by Lynch et al. (2015). The SET pin measurements quantify net surface elevation change, and the MH measurements quantify deposition or accretion above a clay feldspar layer applied on the marsh surface. Vertical accretion is defined as the buildup of mineral and organic sediment on the marsh surface, and elevation change is defined as a change in the height of the wetland surface relative to a local benchmark.

At each study marsh, four SET-MH sites were selected after considering geomorphic setting, surface elevations, and vegetation composition (Figure 1), with two SET-MH plots placed lower in the tide frame and two higher in the tide frame (Table 2). Each SET had three MH paired with it for a total of 4 SETs and 12 MH per marsh site following standardized methods (Cahoon et al., 2020; Webb et al., 2013). SET-MHs were measured during quarterly site visits. Measurement of the MH entails removing a small shallow core (plug) of soil using a soil knife, measuring the depth of surface accretion above the feldspar layer, and replacing the plug (Figure 2a). At Miner Slough, we used a cyrocorer to measure feldspar depth due to the large amount of deposited sediment during the study period. Elevation change was measured by attaching the SET instrument to a collar installed at the top of the local benchmark, in this case the top of the deep rod. The SET instrument provides a constant reference plane in space from which the distance to the marsh surface can be measured. Nine pins are lowered to the surface in 490-degree cardinal directions yielding 36 observations (Figure 2b). Repeat measurements can resolve millimeter-scale change (Cahoon et al., 2002) because the orientation of the table in space remains fixed in time.

Elevation changes and accretion rates were assessed at quarterly intervals (Table S1 in Supporting Information S1). During readings, we determined SET-MH elevations at each site with RTK-GPS as described above. Elevation was converted to a standardized tidal datum,  $z^*$ , where  $z^* = [\text{NAVD88-MSL}]/[\text{MHHW-MSL}]$  (Swanson et al., 2014); using local water level datums, to allow elevation comparisons across sites that have different tide ranges.

#### 2.4. Flooding

At each study site, we deployed Odyssey conductivity sensors (Dataflow Systems Ltd., Christchurch, NZ) to determine the water salinity values over the study period. We also deployed water level loggers (Solinst Levelogger, Georgetown, Ontario, Canada) starting in water year 2015/2016 at all sites except Rush Ranch; for Rush Ranch we used available water data retrieved from San Francisco Bay National Estuarine Research Reserve, First Mallard Branch, (<https://sfbaynerr.sfsu.edu/monitoring-program>). Loggers were deployed near the SET-MHs in

a high-order channel to record as much of the tide range as possible (Figure 1); in all cases, loggers were placed below local MSL to capture all high tides. At Miner Slough, Browns Island, and Rush Ranch, loggers captured the entirety of the tide range. Water loggers recorded water level every 6 min. We serviced loggers to download data and conduct quality checks every 3–4 months. We converted relative water levels into the NAVD88 datum by repeated elevation surveys of the logger housing using RTK GPS and subtracting the distance from the surveyed housing and the logger recorder. At Rush Ranch, we created an offset from a leveled gage (California Department of Water Quality at Belden's Landing), as the gage water level was not available in NAVD88 for the entire time of interest. After conversion, all water level data were then in NAVD88 GEOID12. The data were checked for quality control, including barometric pressure using nearby airport data or additional Solinst loggers that were deployed on-site. Any data gaps in our local records were filled using nearby NOAA or USGS gages and applying site-specific offsets calculated from time periods where gages overlapped (Table S2 in Supporting Information S1).

Provisional mean higher high water (MHHW) and mean high water (MHW) datums were calculated using approximately 5 years of 6-min water data. MLLW was calculated from nearby NOAA gauges to estimate site specific tide ranges, estimated from VDATUM v4.3 (NOAA Vertical Datum Transformation tool), or empirically measured in the field to calculate tide range. MHHW, MHW, and MLLW are vertical tidal datums, which is a reference water level average over a 19-year period. To quantify flooding at each site, we calculated percent time flooded and water depth above MHHW for each SET sampling period ( $n = 12$ , Table S2 in Supporting Information S1). We quantified percent flooding above each datum by summing the number of observations where water levels were above the local datum and dividing that sum by the total number of observations during that SET reading period.

## 2.5. Analysis

To assess how geomorphic setting may influence our results, we ran linear regressions at the site level. Mean cumulative accretion for the entire time period for each site was assessed against each site level covariates reported in Table 1. To test how water levels were altered at each site during the storm sampling period, we compared time flooded and water depths to non-storm time periods (Table S2 in Supporting Information S1) using  $t$ -tests in R ([r-project.org](https://www.r-project.org)). We additionally tested how water levels were altered at each site in the time period directly after the storm period, using the same methods. Storm and post-storm time periods lined up with SET-MH reading periods, so that we could compare water levels and elevation dynamics within the same site-specific time windows.

We used a generalized linear model with Least Absolute Shrinkage and Selection Operator (LASSO) regression to determine which geomorphic factors were the most important predictors in the daily rate of elevation change (R package: `glmnet`, Friedman et al., 2010). LASSO is a regularization technique where the coefficients of unimportant variables are reduced to zero through iterative model fitting. Predictors for each SET-MH included elevation (in  $z^*$ ), distance to San Pablo Bay, distance to the nearest channel, distance to the nearest large (>100 m) channel, and width of the nearest large channel (Table 3 in Supporting Information S1); all predictors were scaled to have a mean of zero and a standard deviation of 1. The analysis was split between storm and non-storm periods.

## 3. Results

### 3.1. Geomorphic and Landscape Setting

The geomorphic landscape setting of each study site was depicted by where they fell within the estuarine gradient, which was comprised of several factors including elevation, tide range, salinity, distance to San Pablo Bay edge, distance and size of the nearest channel, and the size of the nearest major watershed (Table 1). Median elevation for each site showed that Petaluma and Rush Ranch had platforms that were relatively high and within a narrow elevation band, Browns Island and San Pablo had wider elevation distributions, while Miner Slough was relatively low in elevation (Figure S1 in Supporting Information S1). Distance to San Pablo Bay edge was correlated with both tide range and salinity. Petaluma and San Pablo had the greatest tide ranges and salinity; while Rush Ranch, Browns Island and Miner Slough tide ranges and salinities decreased as the sites got further from San Pablo Bay as they became more riverine and freshwater influenced (Table 1). When assessing the influence of the covariates in Table 1 to cumulative sediment accretion over the entire record (January 2016–September



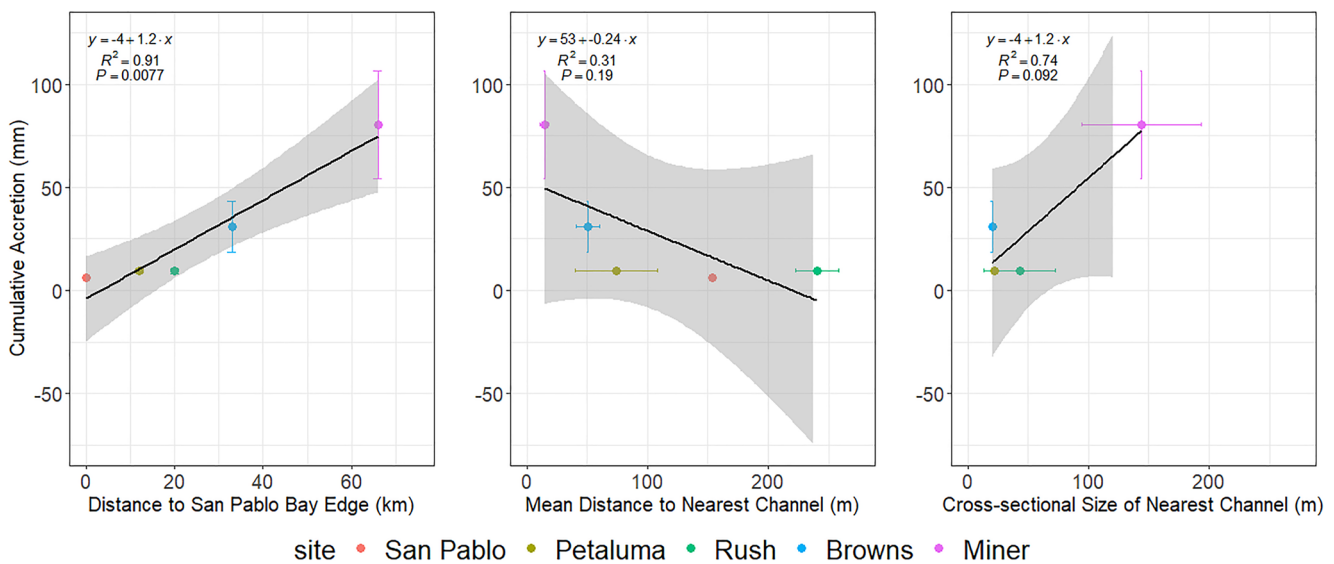


**Figure 3.** Relationship of overall (January 2016–September 2019) cumulative accretion (mean  $\pm$  standard deviation) with geomorphic setting characteristics for each marsh study site for distance to San Pablo Bay edge (left), mean distance to nearest channel (middle), and cross-sectional size of the nearest channel (right). Regression is at the marsh scale with gray area representing the standard deviation. SET-MH mean and standard deviation represented by colored points and lines. Note distance to San Pablo Bay edge is in kilometers.

2019) at the site level, distance to San Pablo Bay edge ( $r^2 = 0.9$ ,  $p = 0.008$ ) and the size of the nearest channel ( $r^2 = 0.74$ ,  $p = 0.09$ ) had the most significant results (Table 1, Figure 3). These factors were further assessed for the storm period (November 2016–March 2017) for their relationship with elevation change at a marsh site level and showed distance to San Pablo Bay edge ( $r^2 = 0.95$ ,  $p = 0.003$ ) and the size of the nearest channel ( $r^2 = 0.85$ ,  $p = 0.05$ ; Table 1, Figure 4) were significant, with distance to nearest channel inversely correlated and less important ( $r^2 = 0.18$ ,  $p = 0.26$ ). Elevation change was used instead of accretion due to missing data at two of the Miner Slough SETs, where sediment addition from the storm was too deep to measure the feldspar layer.

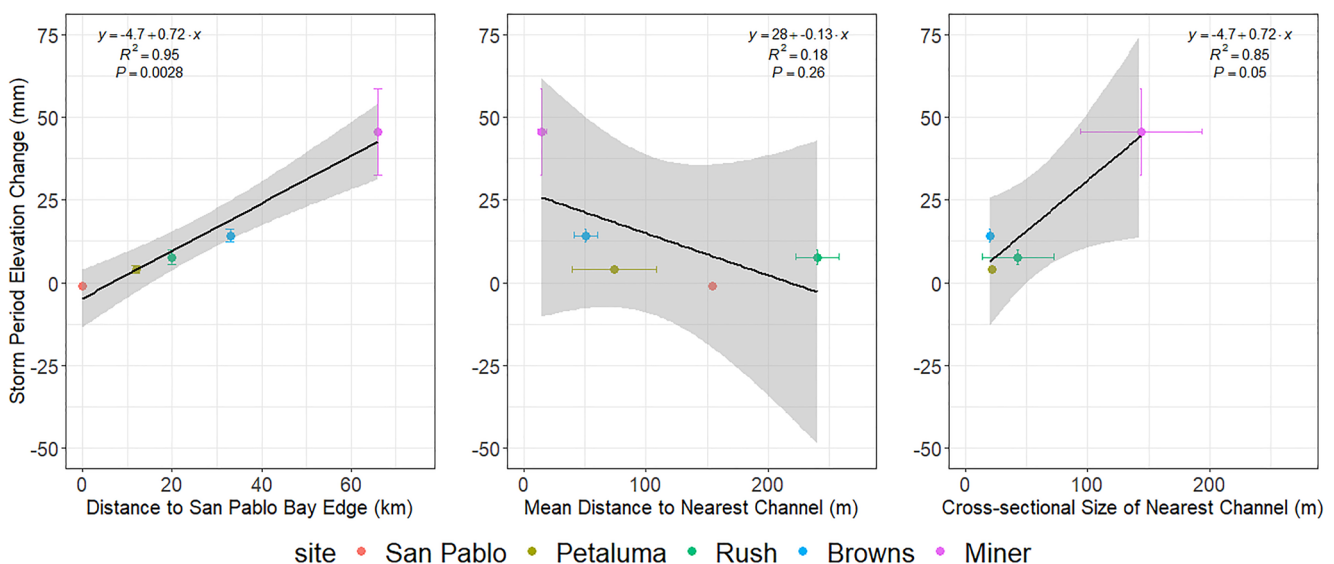


**Figure 4.** Relationship of storm period (November 2016–March 2017) elevation change (mean  $\pm$  standard deviation) with geomorphic setting characteristics for each study site distance to San Pablo Bay edge (left), mean distance to nearest channel (middle), and cross-sectional size of the nearest channel (right). Regression is at the marsh scale with gray area representing the standard deviation. Surface Elevation Table (SET)-marker horizon (MH) mean and standard deviation represented by colored points and lines. Note distance to San Pablo Bay edge is in kilometers.

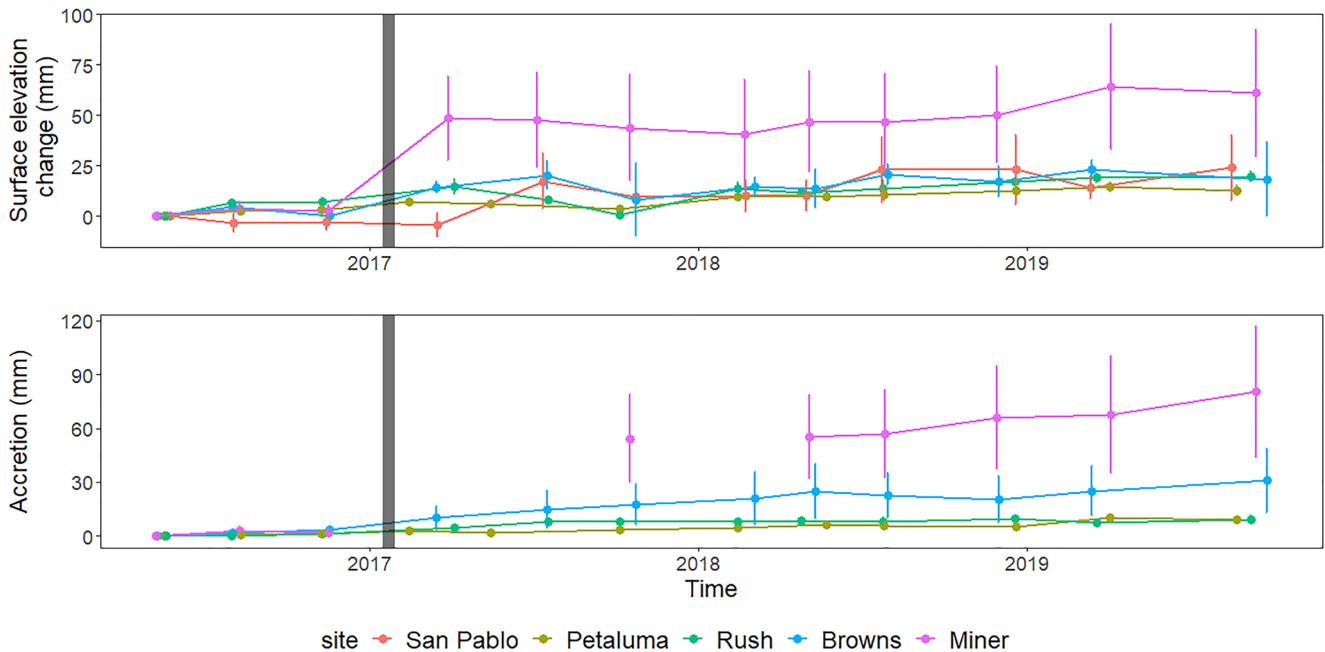


**Figure 5.** Surface elevation change and accretion (mm ± standard error) over time at all sites. Gray vertical line is approximate time of 2017 storm. Note missing data for low Surface Elevation Table (SET)-marker horizon (MH) accretion at San Pablo.

### 3.2. Marsh Accretion and Elevation Change

Total elevation changes and accretion had characteristic patterns across sites in response to the 2017 storm event (Figure 5). Riverine sites response to the storm event was strongest, with Miner Slough having accretion of 11.8–86.0 mm of sediment (Figure 5; mean  $47.5 \pm 19.9$  mm), leading to average surface elevation gains of  $45.6 \pm 13.1$  mm across the site. Browns Island had less accretion after the storm event (Figure 6; 0.9–16 mm; mean  $6.5 \pm 3.5$ ) but still had positive surface elevation gain of  $14.3 \pm 1.8$  mm. We did not detect similar large

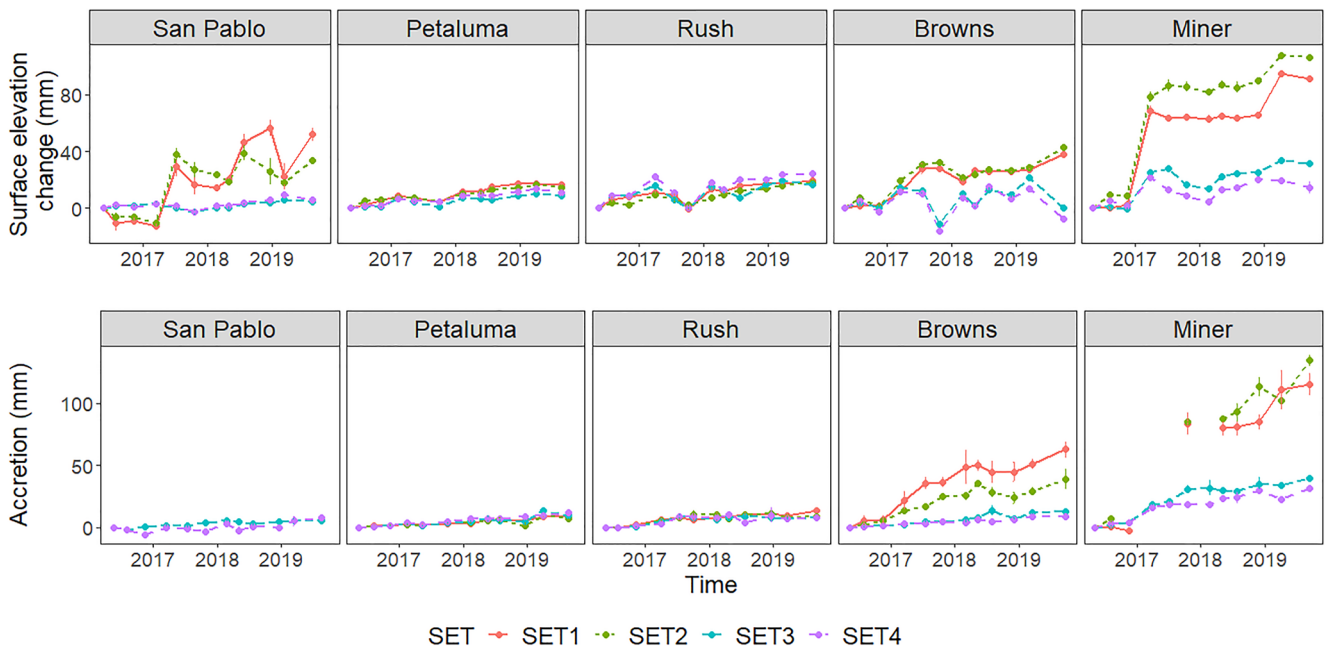


**Figure 6.** Accretion and surface elevation change (mm ± standard error) over time at all sites at Surface Elevation Table (SET)-marker horizon (MH) locations (MH  $n = 3$  per SET). Note missing data for low SET-MH accretion at San Pablo.

storm accretion pulses at Rush Ranch (accretion  $3.1 \pm 0.6$  mm; surface elevation gain  $7.7 \pm 2.2$  mm) or Petaluma (accretion  $1.7 \pm 0.2$  mm; surface elevation gain  $4.0 \pm 1.2$  mm) marshes. San Pablo did not exhibit an immediate response to the storm (Figure 6, accretion from two SETs  $3.2 \pm 2.0$  mm; surface elevation change  $-1.1 \pm 1.6$  mm) but had a surface elevation gain the following measurement period after the storm (03/17/2017–07/12/2017; Figure 6;  $21.5 \pm 13.7$  mm).

SET-MH position in the tidal frame also influenced elevation change ( $z^* = [\text{NAVD88-MSL}]/[\text{MHHW-MSL}]$ ; Figures 5 and 6). Within a marsh, SET-MH plot sites lower in the tidal frame responded more strongly to the storm event than sites higher in the tidal frame. This was evidenced by divergent storm responses in surface elevation change at marshes where large gradients in elevation were present (Figure 6, Figure S1 in Supporting Information S1), including Miner Slough ( $z^*$  range = 0.20–0.88; mean  $45.5 \pm 26.1$  mm; Browns Island ( $z^*$  range = 0.26–0.97; mean  $14.2 \pm 3.5$  mm; and San Pablo ( $z^*$  range = 0.23–1.08; mean  $21.4 \pm 27.4$  [measurement after storm]). In contrast, at Petaluma and Rush Ranch where the high marsh platform elevation is fairly uniform (Figure S1 in Supporting Information S1), SET-MH plots were comparatively higher in the tidal frame and did not respond to the storm event (Figure 5; Rush Ranch:  $z^*$  range = 1.02–1.08, 0.06; mean  $7.6 \pm 4.4$  mm; Petaluma:  $z^*$  range = 0.94–1.03, 0.09; mean  $4.0 \pm 2.3$  mm).

### 3.3. Flooding

Water year 2017 (1 October 2016–30 September 2017) had one of the highest monthly water levels over the last 50 years at the San Francisco NOAA tide gage station, on par with large El Niño events in Water Year (WY)84 and WY98 (Figure 7). During the heaviest precipitation period (January and February 2017; Wen et al., 2018), water levels showed a clear flood signal upstream (Figure 7), with decreasing riverine signal downstream where tidal forcing became dominant. Miner Slough was flooded above local MHHW for several weeks in February, by more than 1 m for days at a time (Figure 7).

The dissipation of water level across the estuary from the riverine sites to the oceanic sites led to differential impacts on the percentage of time the site was flooded above non-storm conditions, with the riverine site being the most flooded during the storm period (Figure 8). All sites had increased percent time flooded during the storm SET-MH measurement period compared to baseline conditions (Figure 8;  $P < 0.01$  in all cases). However, the magnitude of excess percentage time flooded sharply decreased from riverine to bay sites (Figures 7 and 8; 35% inundation [ $P < 0.001$ ], 55 cm water depth [ $P < 0.001$ ] Miner Slough; 11% inundation [ $P < 0.001$ ], 10 cm water depth [ $P < 0.001$ ] Browns Island; 5% inundation [ $P = 0.003$ ], 5 cm water depth [ $P < 0.001$ ] Rush Ranch; 6% inundation [ $P < 0.001$ ], 5 cm water depth [ $P < 0.001$ ] Petaluma; 3% inundation [ $P = 0.004$ ], 4 cm water depth [ $P = 0.001$ ] San Pablo). Storm-induced flooding was not detected during the following SET-MH measurement period over the summer 2017, except for the riverine site Miner Slough (4% above baseline inundation  $P = 0.004$ ; 4 cm excess water depth  $P = 0.006$ ).

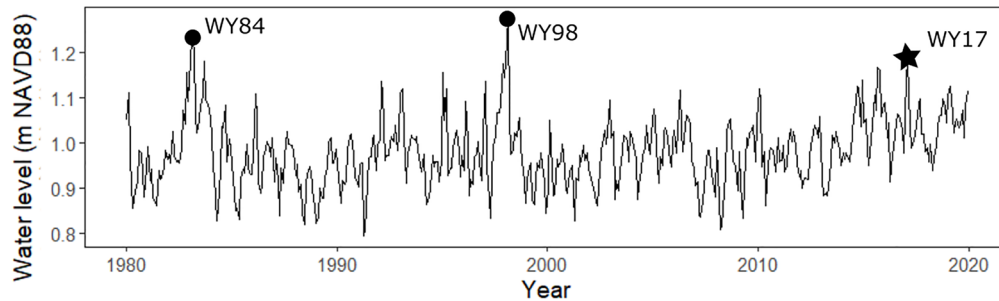
During the storm period, distance to San Pablo Bay was the strongest predictor of elevation change, followed by SET-MH elevation; none of the other predictors (width and distance of nearest large channel and nearest channel distance) were important with coefficients shrunk to zero (Figure 9). Conversely, during non-storm periods, elevation was a relatively strong predictor, followed by the width of the nearest large channel, distance to nearest large channel, and then distance to San Pablo Bay; distance to nearest channel of any size was not important. The  $r^2$  were 0.70 and 0.75 for the storm and non-storm period models, respectively. Data used for this analysis can be found at Thorne et al. (2022).

## 4. Discussion

### 4.1. Geomorphic and Landscape Settings

While storms and associated flooding can have adverse effects on human infrastructure and economies, they can also generate beneficial effects for marshes if they build elevations (Smith et al., 2015). Our results demonstrate how naturally occurring, but infrequent storms can shape estuaries and marsh sedimentary dynamics, but those influences varied across spatial scales and settings within the estuary. For the San Francisco Bay-Delta, our results illustrate the importance of the riverine watershed for sediment delivery to marshes along the Sacramento River, Suisun Bay, and San Pablo Bay during AR events. Future sediment supply from the Sacramento and San

A



B

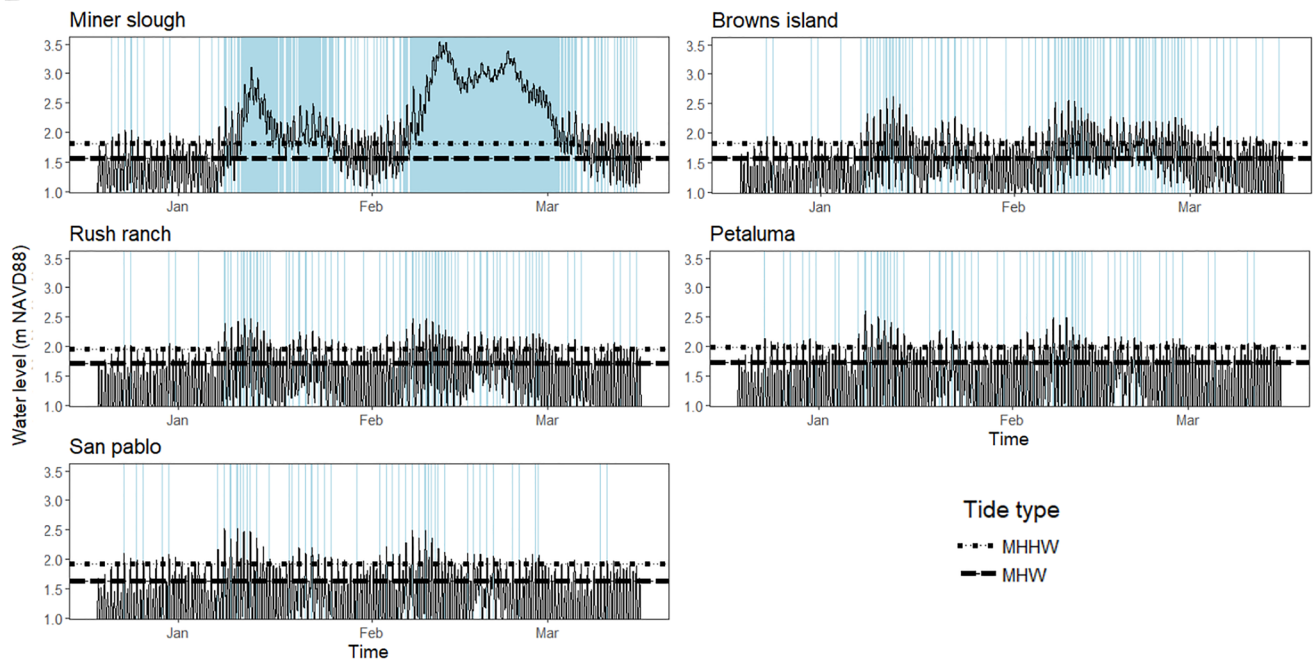


**Figure 7.** (a) Monthly average water level at the Golden Gate Bridge (NOAA tide gauge) with three highest monthly water levels highlighted. Elevated water levels in Water Year (WY)84 and WY98 were due to El Niño, while WY17 is the focus of this paper. (b) Hydrograph at each study site during the heaviest precipitation during the first 3 months of 2017 (Wen et al., 2018), from riverine to ocean influence: Miner Slough, Browns Island, Rush Ranch, Petaluma, and San Pablo. Blue shading in panel B represents the amount of time water levels were above local MHHW at each site. All sites experienced elevated water levels during the storm periods.

Joaquin River Delta is uncertain, but anthropogenic activities throughout the Delta watershed have decreased suspended sediment availability by about 50% between 1957 and 2001 to San Francisco Bay because of trapping of sediment in reservoirs, armoring of riverbanks, levee development, and land conversion (Wright & Schoellhamer, 2004). Our results are of particular importance for other estuaries that are also experiencing reduced sediment supply, such as the Yangtze River delta in China (Yang, 2005) and the Mediterranean drainage basin (Poulos & Collins, 2002), which are experiencing loss of sediment discharge related to dam developments. Storm waters and associated suspended sediment may become trapped behind dams and other infrastructure on rivers, preventing their delivery to tidal marshes.

When assessing the geomorphic and landscape setting of the marsh study sites within the estuary, we determined that during non-storm periods, elevation and distance from channels were important in controlling elevation change (Table 1, Figure 9). These non-storm results aligned with Buffington et al. (2020) who also found that mineral deposition on the marsh surface varied by distance from channels and size of channels at Rush Ranch and Petaluma. Our results showed that distance from San Pablo Bay and SET-MH elevations also played important roles in the AR influence on elevation change. The prolonged hydroperiod related to storm flooding in the upper portions of the estuary essentially overwhelmed the usual tidal relationship between channel size and distance

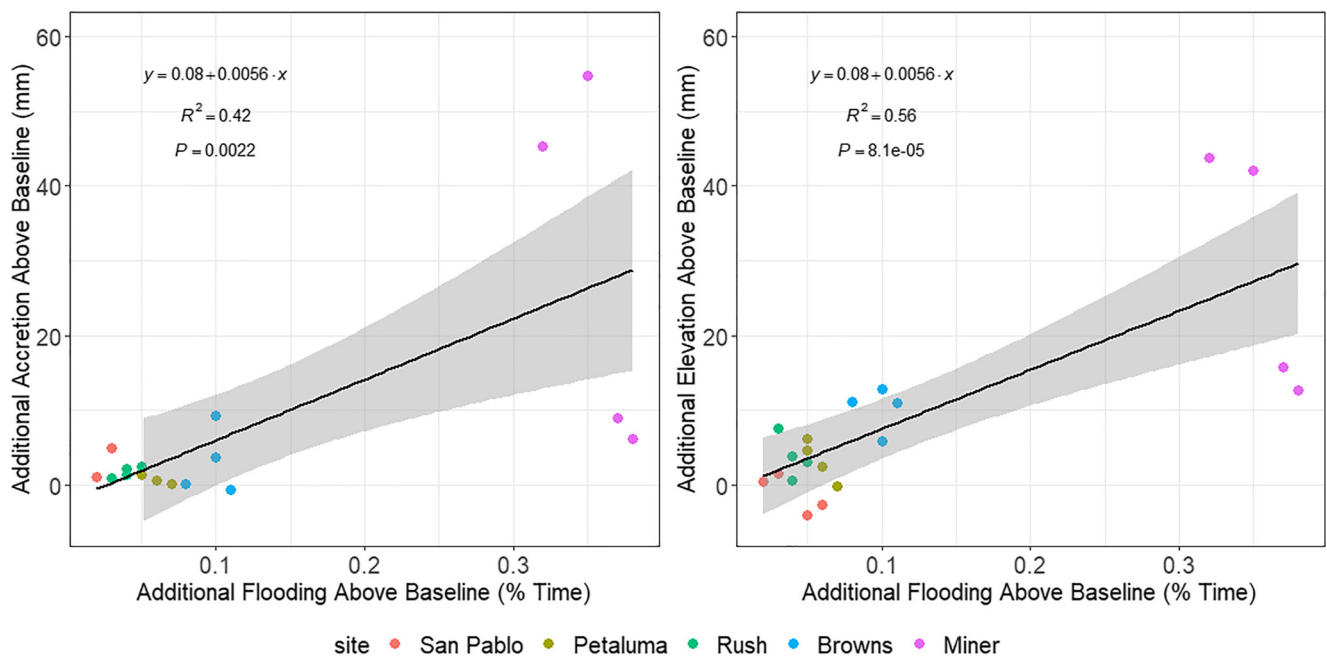


**Figure 8.** The relationship between accretion (mm) and percent time flooded for all marsh sites and Surface Elevation Table (SET)-marker horizon (MH) locations (left), and the relationship between total elevation change and time flooded for all marsh sites and SET-MH locations (right). Each point is a SET-MH location at that marsh, during the storm period.

on marsh deposition. The importance of hydroperiod and channels on short term marsh accretion has also been documented (Reed et al., 1999); however, during the storm events, we found that the change in hydroperiod was primarily related to the location within the estuary and was not related to elevation distribution or mean marsh elevation as would normally be expected.

We also measured an increase in flooding time across all the study sites in the estuary due to the AR, but not a direct 1:1 relationship with accretion and elevation change. However, only the marsh site that was primarily riverine influenced had a clear accretion signal related to prolonged flooding (Figure 8), illustrating the importance of suspended sediment concentrations and proximity to sediment sources in regulating accretion rates. The Hudson River watershed had similar response where sediment was predominantly trapped in the tidal freshwater wetlands in the wake of tropical storms Irene and Lee and was not transported to the lower estuary as expected (Ralston et al., 2013). Our study did not monitor suspended sediment concentrations explicitly during the storm period; however, monitoring stations exist throughout the estuary. A turbidity sensor located near Miner Slough had a maximum 122 NTU of turbidity during WY2017 with prolonged higher concentrations when compared with other years (station: B9147000; Figure S2a in Supporting Information S1). Similar patterns were seen at a turbidity monitoring station at Rush Ranch where there was elevated turbidity with a peak near 160 NTU, but overall trends were similar when compared with other years (Figure S2b in Supporting Information S1). Relationships between ARs and changes in turbidity and suspended sediment within an estuary need to be assessed to fully understand storm effects on marsh accretion processes. We expect this pattern to vary greatly in other estuaries depending on the origin of the storm and whether the geomorphic setting is riverine dominated or not.

#### 4.2. Storm Ecological Impacts

ARs occur during all seasons over the North Pacific and frequently occur in the Aleutian Islands, Japan, and U.S. Pacific Coast, but many do not make landfall (Mundhenk et al., 2016). However, ARs are responsible for transporting large amounts of water creating extreme precipitation and wind events when they do reach land. ARs have been documented to create strong low level winds that can have more than double the wind speeds of all other storm conditions in the same location (Gimeno et al., 2014; Waliser & Guan, 2017), illustrating their importance as large infrequent disturbances to coastlines. At our study sites, we did not observe scour or erosion indicative of soil loss; however, marshes that are more exposed to fast flowing waters or extreme winds during

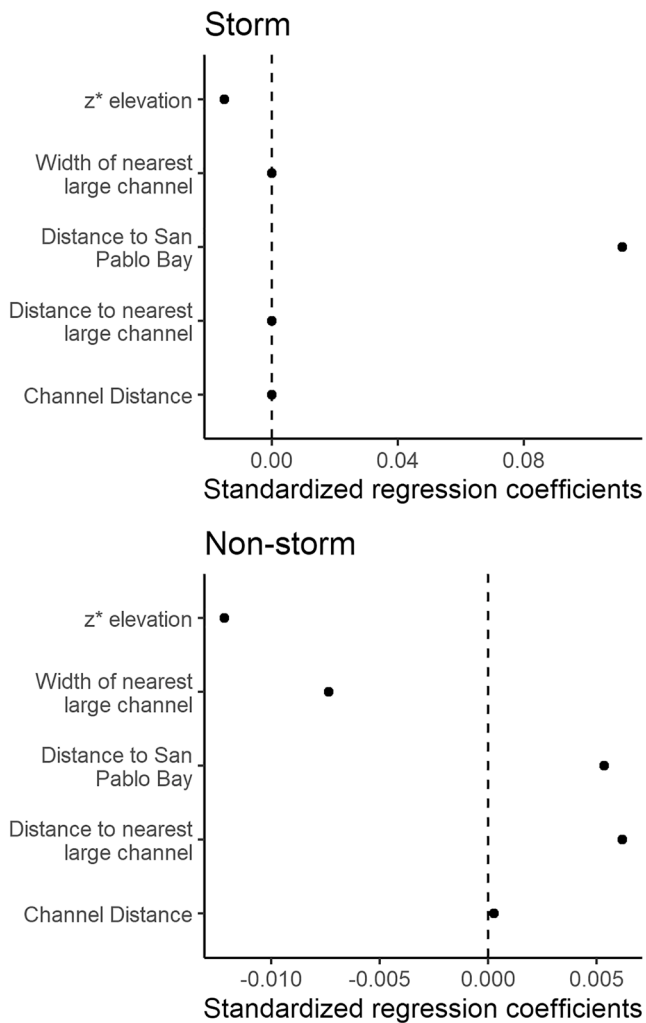


**Figure 9.** Standardized regression coefficients for models relating elevation change to geomorphic factors. Distance to San Pablo Bay was the most important predictor of elevation change during the storm period, with elevation of the Surface Elevation Table (SET)-marker horizon (MH) as the second most important. During the non-storm time period everything except distance to the nearest channel was a predictor of elevation change.

storms could experience edge and surface erosion which could decrease surface elevations offsetting any deposition gains. Wind can also resuspend sediments from adjacent mudflats and mobilize sediments for deposition on the marsh surface during a storm. Our measurements showed an increase in surface elevation at the San Pablo Bay marsh lower elevations following the peak storm but not during the storm period itself, suggesting a delay in deposition on the surface possibly from resuspension of the nearby mudflat. Mudflat morphodynamic evolution can vary by tidal flow, sediment supply, erodibility, and wave action especially during spring months in San Francisco Bay, but can also be remarkably stable (van der Wegen et al., 2019). This illustrates the need for strong winds or storms to deposit fine sediments in the shallow intertidal area (Ruhl et al., 2004), and resuspend sediments to the marsh surface (Lacy et al., 2020), a topic largely understudied in most estuaries. In this study, we observed the possible importance of adjacent mudflats as sediment reservoirs that can then feed marsh accretion processes long after a storm event.

#### 4.3. Climate Change

Tidal marsh elevation building processes can offset accelerating sea-level rise rates and prevent habitat loss or transition and maintain other ecosystem services (Cahoon et al., 1996; Warren & Niering, 1993; Yellen et al., 2021). Extensive modeling has shown that in many global regions accretion rates are not adequate to outpace relative sea-level rise (Alizad et al., 2018; Fagherazzi et al., 2012; Kirwan et al., 2010; Schile et al., 2014; Stralberg et al., 2011; Swanson et al., 2014; Thorne et al., 2018). However, marshes can trap and retain sediment to build elevations relative to sea-level rise given an adequate supply. In the Tijuana Estuary, it was documented that accretion in the low marsh was attributed to episodic storm induced river flows during the winter of 1993 (Cahoon et al., 1996), creating “elevation capital” (Cahoon & Guntenspergen, 2010) relative to local sea levels. At three of our sites, we observed a significant increase in marsh elevation following the storm that provided “elevation capital” when compared with relative sea-level rise, presumably reducing submergence risk. Here, ARs may provide an opportunity for positive elevation trajectories to offset sea-level rise at some locations, but more research is needed to fully understand sediment deposition and erosion rates, storm surge-related soil compaction, and potential negative plant feedbacks.

Incorporating accretion responses due to ARs and other storms may improve model projections of marsh responses to sea-level rise. Many popular modeling approaches for marsh response to sea-level rise use multi-annual averages or ranges of suspended sediment concentrations that don't reflect changes to suspended sediment concentration due to infrequent storms (Byrd et al., 2016; Schile et al., 2014; Stralberg et al., 2011). Also, models calibrated with dated soil cores (e.g., Buffington et al., 2021; Thorne et al., 2018) implicitly assume stationarity in the frequency and intensity of storms and ARs. However, climate change may cause ARs to change in frequency and intensity delivering more precipitation (Espinoza et al., 2018; Payne et al., 2020). The next generation of wetland evolution models should explicitly account for future non-stationarity to better understand whether future ARs may increase or decrease sea-level rise marsh resilience. Also, episodic variation in precipitation influences suspended sediment concentrations, which can be used to directly inform marsh modeling (Temmerman et al., 2003). Model explorations of tide range and accretion indicate that high marsh platforms are particularly dependent on infrequent storms for sediment deposition (Goodwin & Mudd, 2019). Long-term monitoring of SET-MH is one of the most robust approaches for gathering the necessary data to constrain such modeling efforts.

Understanding the impacts of storms and their interactions with marsh vegetation, sediment dynamics, and elevation is important when trying to evaluate marsh long-term resilience under a changing climate. Climate change may affect the frequency, intensity, and geographic distribution of AR storms (Dettinger, 2011; Ramos et al., 2016), which is becoming increasingly more documented (Chen et al., 2019; Lavers et al., 2011; Lyngwa & Nayak, 2021; Paltan et al., 2017). Global warming could impact AR characteristics that shape water supply and hydroclimate risks, including observed increases in water vapor transport (Gershunov et al., 2017), changes to the frequency of AR events (Gao et al., 2015; Ramos et al., 2016; Shields & Kiehl, 2016), and increase in extreme precipitation associated with ARs (Hagos et al., 2016). Surface air temperatures during California ARs are projected to increase about 2°C (Dettinger, 2011), which could result in warmer air conditions during AR events and more extreme precipitation. Gonzales et al. (2019) found that between 1980 and 2016, landfall AR temperatures have increased up to 2°C with the most robust warming occurring in November and March, which could lead to shifts from snow to more rain. Ramos et al. (2016) projected more intense precipitation and floods along the Atlantic European Coasts from ARs under climate change scenarios. Another study suggests that ARs would increase in frequency and total precipitation in British Columbia, Canada with a northward shift in landfalls (Radić et al., 2015). The changing nature of ARs and extreme precipitation events make it difficult to fully understand how they will influence estuarine ecosystems and marsh processes in the near and long-term.

## 5. Conclusion

As global temperatures increase and storm intensity and frequency change, the impacts of episodic disturbance to estuaries and marsh processes become less clear. We know a great deal about the impacts to coastal ecosystems and marshes from hurricanes and tropical cyclones, but assessments of other large infrequent storm events, like ARs, with prolonged precipitation events and flooding are lacking in the literature. Here, we demonstrate the usefulness of a long-term monitoring approach (Surface Elevation Tables-Marker Horizons) to understand sediment delivery patterns to marshes across an estuarine gradient during an extreme AR event. Expanding this monitoring approach across different types of estuaries globally that experience ARs especially under a changing climate, could be valuable. Our results illustrate the importance of marsh geomorphic and landscape setting in mediating deposition and flooding from the storms within the estuarine landscape. More work is needed to fully understand how a changing climate will influence the intensity and frequency of extreme storm events and their potential impacts to tidal wetland ecosystem processes and persistence. A better understanding of how sea-level rise and future extreme weather events will affect marshes will aid future management of tidal wetlands.

## Acknowledgments

Funding was provided by U.S. Geological Survey Priority Ecosystem Science Program. The authors would like to thank the U.S. Geological Survey, Western Ecological Research Center & Eastern Ecological Science Center for support. CJ would like to acknowledge support from NOAA Effects of Sea Level Rise Program. National Oceanic and Atmospheric Administration (NOAA) GRG acknowledges support from the Ecosystem Mission Area, Land Change Science (Climate R&D) Program. Site access was provided by the California Department of Fish and Wildlife Service (K. Taylor), U.S. Fish and Wildlife Service (D. Brubaker, M. Marriott, M. Amato, L. Terrazas), Rush Ranch NERR (M. Vasey, M. Ferner), Solano Land Trust, and East Bay Regional Parks. We would like to thank field staff including A. Kennedy, K. Backe, K. Mosher, A. Goodman, and V. Corbet. The authors declare that they have no conflict of interest. Any use of trade, product, or firm names in this publication is for descriptive purposes only and does not imply endorsement by the U.S. Government.

## Data Availability Statement

Water and Surface Elevation Table-Marker Horizon data were made available at [sciencebase.gov](https://sciencebase.gov) at <https://doi.org/10.5066/P95UFMIS>.

## References

- Alizad, K., Hagen, S. C., Medeiros, S. C., Bilskie, M. V., Morris, J. T., Balthis, L., & Buckel, C. A. (2018). Dynamic responses and implications to coastal wetlands and the surrounding regions under sea level rise. *PLoS One*, *13*, e0205176. <https://doi.org/10.1371/journal.pone.0205176>
- Alizad, K., Hagen, S. C., Morris, J. T., Medeiros, S. C., Bilskie, M. V., & Weishampel, J. F. (2016). Coastal wetland response to sea-level rise in a fluvial estuarine system. *Earth's Future*, *4*, 483–497. <https://doi.org/10.1002/2016EF000385>
- American Meteorological Society. (2018). *Atmospheric river*. Glossary of Meteorology.
- Barnard, P. L., Erikson, L. H., Foxgrover, A. C., Hart, J. A. F., Limber, P., O'Neill, A. C., et al. (2019). Dynamic flood modeling essential to assess the coastal impacts of climate change. *Scientific Reports*, *9*, 4309. <https://doi.org/10.1038/s41598-019-40742-z>
- Buffington, K. J., Dugger, B. D., Thorne, K. M., & Takekawa, J. Y. (2016). Statistical correction of lidar-derived digital elevation models with multispectral airborne imagery in tidal marshes. *Remote Sensing of Environment*, *186*, 616–625. <https://doi.org/10.1016/j.rse.2016.09.020>
- Buffington, K. J., Goodman, A. C., Freeman, C. M., & Thorne, K. M. (2020). Testing the interactive effects of flooding and salinity on tidal marsh plant productivity. *Aquatic Botany*, *164*, 103231. <https://doi.org/10.1016/j.aquabot.2020.103231>
- Buffington, K. J., Janousek, C. N., Dugger, B. D., Callaway, J. C., Schile-Beers, L. M., Borgnis Sloane, E., & Thorne, K. M. (2021). Incorporation of uncertainty to improve projections of tidal wetland elevation and carbon accumulation with sea-level rise. *Plos ONE*, *16*, e0256707. <https://doi.org/10.1371/journal.pone.0256707>
- Buffington, K. J., & Thorne, K. M. (2019). *LEAN-corrected San Francisco Bay digital elevation model, 2018*. <https://doi.org/10.5066/P97J9GUG>
- Buffington, K. J., Thorne, K. M., Takekawa, J. Y., Chappell, S., Swift, T., Feldheim, C., et al. (2019). *LEAN-corrected DEM for Suisun Marsh*. <https://doi.org/10.5066/P97R4ES3>
- Byrd, K. B., Windham-Myers, L., Leeuw, T., Downing, B., Morris, J. T., & Ferner, M. C. (2016). Forecasting tidal marsh elevation and habitat change through fusion of Earth observations and a process model. *Ecosphere*, *7*. <https://doi.org/10.1002/ecs2.1582>
- Cahoon, D., & Guntenspergen, G. (2010). Climate change, sea-level rise, and coastal wetlands. *National Wetlands Newsletter*, *32*, 8–12.

- Cahoon, D. R. (2006). A review of major storm impacts on coastal wetland elevations. *Estuaries and Coasts*, 29, 889–898. <https://doi.org/10.1007/BF02798648>
- Cahoon, D. R., Lynch, J. C., Perez, B. C., Segura, B., Holland, R. D., Stelly, C., et al. (2002). High-precision measurements of wetland sediment elevation: II. The rod surface elevation table. *Journal of Sediment Research*, 72, 734–739. <https://doi.org/10.1306/020702720734>
- Cahoon, D. R., Lynch, J. C., & Powell, A. N. (1996). Marsh vertical accretion in a southern California estuary. *U.S.A. Estuarine, Coastal and Shelf Science*, 43, 19–32. <https://doi.org/10.1006/ecss.1996.0055>
- Cahoon, D. R., Reed, D. J., Day, J. W., Lynch, J. C., Swales, A., & Lane, R. R. (2020). Applications and utility of the surface elevation table–marker horizon method for measuring wetland elevation and shallow soil subsidence–expansion: Discussion/reply to: Byrnes M., Britsch L., Berlinghoff J., Johnson R., and Khalil S. 2019. Recent subsidence rates for Barataria Basin, Louisiana. *Geo-Marine Letters* 39:265–815. <https://doi.org/10.1007/s00367-020-00656-6>
- Cahoon, D. R., & Turner, R. E. (1989). Accretion and canal impacts in a rapidly subsiding wetland II. Feldspar marker horizon technique. *Estuaries*, 12, 260. <https://doi.org/10.2307/1351905>
- Carvajal, M., Winckler, P., Garreaud, R., Iguale, F., Contreras-López, M., Averil, P., et al. (2021). Extreme sea levels at Rapa Nui (Easter Island) during intense atmospheric rivers. *Natural Hazards*, 106, 1619–1637. <https://doi.org/10.1007/s11069-020-04462-2>
- Castelle, B., Marieu, V., Bujan, S., Splinter, K. D., Robinet, A., Sénéchal, N., & Ferreira, S. (2015). Impact of the winter 2013–2014 series of severe Western Europe storms on a double-barred sandy coast: Beach and dune erosion and megacusp embayments. *Geomorphology*, 238, 135–148. <https://doi.org/10.1016/j.geomorph.2015.03.006>
- Chen, X., Leung, L. R., Wigmosta, M., & Richmond, M. (2019). Impact of atmospheric rivers on surface hydrological processes in Western U.S. Watersheds. *Journal of Geophysical Research: Atmospheres*, 124, 8896–8916. <https://doi.org/10.1029/2019JD030468>
- Cloern, J. E., & Jassby, A. D. (2012). Drivers of change in estuarine-coastal ecosystems: Discoveries from four decades of study in San Francisco Bay. *Reviews of Geophysics*, 50, RG4001. <https://doi.org/10.1029/2012RG000397>
- Correll, M. D., Wiest, W. A., Hodgman, T. P., Shriver, W. G., Elphick, C. S., McGill, B. J., et al. (2017). Predictors of specialist avifaunal decline in coastal marshes: Avian Decline in Tidal Marshes. *Conservation Biology*, 31, 172–182. <https://doi.org/10.1111/cobi.12797>
- Craft, C., Clough, J., Ehman, J., Joye, S., Park, R., Pennings, S., et al. (2009). Forecasting the effects of accelerated sea-level rise on tidal marsh ecosystem services. *Frontiers in Ecology and the Environment*, 7, 73–78. <https://doi.org/10.1890/070219>
- Dale, V., Lugo, A., MacMahon, J., & Pickett, S. (1998). Ecosystem management in the context of large, infrequent disturbances. *Ecosystems*, 1, 546–557. <https://doi.org/10.1007/s100219900050>
- Day, J. W., Pont, D., Hensel, P. F., Ibañez, C., & Ibanez, C. (1995). Impacts of sea-level rise on deltas in the Gulf of Mexico and the Mediterranean: The importance of pulsing events to sustainability. *Estuaries*, 18, 636. <https://doi.org/10.2307/1352382>
- Dettinger, M. (2011). Climate change, atmospheric rivers, and floods in California - a Multimodel analysis of storm frequency and magnitude Changes I: Climate change, atmospheric rivers, and floods in California - a Multimodel analysis of storm frequency and magnitude changes. *JAWRA Journal of American Water Resources Association*, 47, 514–523. <https://doi.org/10.1111/j.1752-1688.2011.00546.x>
- Dettinger, M. D. (2013). Atmospheric rivers as drought busters on the U.S. West coast. *Journal of Hydrometeorology*, 14, 1721–1732. <https://doi.org/10.1175/JHM-D-13-02.1>
- Espinoza, V., Waliser, D. E., Guan, B., Lavers, D. A., & Ralph, F. M. (2018). Global analysis of climate change projection effects on atmospheric rivers. *Geophysical Research Letters*, 45, 4299–4308. <https://doi.org/10.1029/2017GL076968>
- Fagherazzi, S., Kirwan, M. L., Mudd, S. M., Guntenspergen, G. R., Temmerman, S., D'Alpaos, A., et al. (2012). Numerical models of salt marsh evolution: Ecological, geomorphic, and climatic factors. *Reviews of Geophysics*, 50, RG1002. <https://doi.org/10.1029/2011RG000359>
- Feher, L. C., Osland, M. J., Anderson, G. H., Vervaeke, W. C., Krauss, K. W., Whelan, K. R. T., et al. (2020). The long-term effects of hurricanes Wilma and Irma on soil elevation change in Everglades mangrove forests. *Ecosystems*, 23, 917–931. <https://doi.org/10.1007/s10021-019-00446-x>
- Friedman, J., Hastie, T., & Tibshirani, R. (2010). Regularization paths for generalized linear models via coordinate descent. *Journal of Statistical Software*, 33. <https://doi.org/10.18637/jss.v033.i01>
- Gao, Y., Lu, J., Leung, L. R., Yang, Q., Hagos, S., & Qian, Y. (2015). Dynamical and thermodynamical modulations on future changes of landfalling atmospheric rivers over Western North America. *Geophysical Research Letters*, 42, 7179–7186. <https://doi.org/10.1002/2015GL065435>
- Gershunov, A., Shulgina, T., Ralph, F. M., Lavers, D. A., & Rutz, J. J. (2017). Assessing the climate-scale variability of atmospheric rivers affecting Western North America: Atmospheric River Climate-Scale Behavior. *Geophysical Research Letters*, 44, 7900–7908. <https://doi.org/10.1002/2017GL074175>
- Gimeno, L., Nieto, R., Vázquez, M., & Lavers, D. A. (2014). Atmospheric rivers: A mini-review. *Frontiers of Earth Science*, 2. <https://doi.org/10.3389/feart.2014.00002>
- Gonzales, K. R., Swain, D. L., Nardi, K. M., Barnes, E. A., & Diffenbaugh, N. S. (2019). Recent warming of landfalling atmospheric rivers along the west coast of the United States. *Journal of Geophysical Research: Atmospheres*, 124(13), 6810–6826. <https://doi.org/10.1029/2018JD029860>
- Goodman, A. C., Thorne, K. M., Buffington, K. J., Freeman, C. M., & Janousek, C. N. (2018). El Niño increases high-tide flooding in tidal wetlands along the U.S. Pacific coast. *Journal of Geophysical Research: Biogeosciences*, 123, 3162–3177. <https://doi.org/10.1029/2018JG004677>
- Goodwin, G. C. H., & Mudd, S. M. (2019). High platform elevations highlight the role of storms and spring tides in salt marsh evolution. *Frontiers in Environmental Science*, 7, 62. <https://doi.org/10.3389/fevs.2019.00062>
- Guntenspergen, G. R., Cahoon, D. R., Grace, J., Steyer, G. D., Fournet, S., Townson, M. A., & Foote, A. L. (1995). Disturbance and recovery of the Louisiana coastal marsh landscape from the impacts of hurricane Andrew. *Journal of Coastal Research*, 324–339.
- Hagos, S. M., Leung, L. R., Yoon, J., Lu, J., & Gao, Y. (2016). A projection of changes in landfalling atmospheric river frequency and extreme precipitation over Western North America from the Large Ensemble CESM simulations. *Geophysical Research Letters*, 43, 1357–1363. <https://doi.org/10.1002/2015GL067392>
- Harvey, M. E., Giddings, S. N., Stein, E. D., Crooks, J. A., Whitcraft, C., Gallien, T., et al. (2020). Effects of elevated sea levels and waves on southern California estuaries during the 2015–2016 El Niño. *Estuaries and Coasts*, 43, 256–271. <https://doi.org/10.1007/s12237-019-00676-1>
- Hauser, S., Meixler, M. S., & Laba, M. (2015). Quantification of impacts and ecosystem services loss in New Jersey coastal wetlands due to hurricane sandy storm surge. *Wetlands*, 35, 1137–1148. <https://doi.org/10.1007/s13157-015-0701-z>
- Hensel, P. F., Day, J. W., Pont, D., & Day, J. N. (1998). Short-term sedimentation dynamics in the Rhône River delta, France: The importance of riverine pulsing. *Estuaries*, 21, 52. <https://doi.org/10.2307/1352546>
- Janousek, C., Buffington, K., Thorne, K., Guntenspergen, G., Takekawa, J., & Dugger, B. (2016). Potential effects of sea-level rise on plant productivity: Species-specific responses in northeast Pacific tidal marshes. *Marine Ecology Progress Series*, 548, 111–125. <https://doi.org/10.3354/meps11683>
- Janousek, C. N., Thorne, K. M., & Takekawa, J. Y. (2019). Vertical zonation and niche breadth of tidal marsh plants along the northeast Pacific coast. *Estuaries and Coasts*, 42, 85–98. <https://doi.org/10.1007/s12237-018-0420-9>



- Kirwan, M. L., & Guntenspergen, G. R. (2015). Response of plant productivity to experimental flooding in a stable and a submerging marsh. *Ecosystems*, *18*, 903–913. <https://doi.org/10.1007/s10021-015-9870-0>
- Kirwan, M. L., Guntenspergen, G. R., D'Alpaos, A., Morris, J. T., Mudd, S. M., & Temmerman, S. (2010). Limits on the adaptability of coastal marshes to rising sea level: Ecogeomorphic limits to wetland survival. *Geophysical Research Letters*, *37*. <https://doi.org/10.1029/2010gl045489>
- Kirwan, M. L., Murray, A. B., & Boyd, W. S. (2008). Temporary vegetation disturbance as an explanation for permanent loss of tidal wetlands. *Geophysical Research Letters*, *35*, L05403. <https://doi.org/10.1029/2007GL032681>
- Lacy, J. R., Foster-Martinez, M. R., Allen, R. M., Ferner, M. C., & Callaway, J. C. (2020). Seasonal variation in sediment delivery across the bay-marsh interface of an estuarine salt marsh. *Journal of Geophysical Research: Oceans*, *125*. <https://doi.org/10.1029/2019JC015268>
- Langston, A. K., Coleman, D. J., Jung, N. W., Shawler, J. L., Smith, A. J., Williams, B. L., et al. (2021). The effect of marsh age on ecosystem function in a rapidly transgressing marsh. *Ecosystems*. <https://doi.org/10.1007/s10021-021-00652-6>
- Larkin, D. J., Madon, S. P., West, J. M., & Zedler, J. B. (2008). Topographic heterogeneity influences fish use of an experimentally restored tidal marsh. *Ecological Applications*, *18*, 483–496. <https://doi.org/10.1890/06-1984.1>
- Lavers, D. A., Allan, R. P., Wood, E. F., Villarini, G., Brayshaw, D. J., & Wade, A. J. (2011). Winter floods in Britain are connected to atmospheric rivers: UK winter floods and atmospheric rivers. *Geophysical Research Letters* *38*. <https://doi.org/10.1029/2011gl049783>
- Lavers, D. A., & Villarini, G. (2015). The contribution of atmospheric rivers to precipitation in Europe and the United States. *Journal of Hydrology*, *522*, 382–390. <https://doi.org/10.1016/j.jhydrol.2014.12.010>
- Lynch, J., Hensel, P., & Cahoon, D. (2015). *The surface elevation table and marker horizon technique: A protocol for monitoring wetland elevation dynamics*. <https://doi.org/10.13140/RG.2.1.5171.9761>
- Lyngwa, R. V., & Nayak, M. A. (2021). Atmospheric river linked to extreme rainfall events over Kerala in August 2018. *Atmospheric Research*, *253*, 105488. <https://doi.org/10.1016/j.atmosres.2021.105488>
- McKee, K. L., & Cherry, J. A. (2009). Hurricane Katrina sediment slowed elevation loss in subsiding brackish marshes of the Mississippi River delta. *Wetlands* *29*, 2–15. <https://doi.org/10.1672/08-32.1>
- McKee, L. J., Lewicki, M., Schoellhamer, D. H., & Ganju, N. K. (2013). Comparison of sediment supply to San Francisco bay from watersheds draining the bay area and the central valley of California. *Marine Geology*, *345*, 47–62. <https://doi.org/10.1016/j.margeo.2013.03.003>
- Merkens, J.-L., Reimann, L., Hinkel, J., & Vafeidis, A. T. (2016). Gridded population projections for the coastal zone under the Shared Socioeconomic Pathways. *Global and Planetary Change*, *145*, 57–66. <https://doi.org/10.1016/j.gloplacha.2016.08.009>
- Moore, L. J., & Griggs, G. B. (2002). Long-term cliff retreat and erosion hotspots along the central shores of the Monterey Bay National Marine Sanctuary. *Marine Geology*, *181*, 265–283. [https://doi.org/10.1016/S0025-3227\(01\)00271-7](https://doi.org/10.1016/S0025-3227(01)00271-7)
- Morton, R. A., & Barras, J. A. (2011). Hurricane impacts on coastal wetlands: A half-century record of storm-generated features from southern Louisiana. *Journal of Coastal Research*, *275*, 27–43. <https://doi.org/10.2112/JCOASTRES-D-10-00185.1>
- Mundhenk, B. D., Barnes, E. A., & Maloney, E. D. (2016). All-season climatology and variability of Atmospheric River frequencies over the north Pacific. *Journal of Climate*, *29*, 4885–4903. <https://doi.org/10.1175/JCLI-D-15-0655.1>
- NOAA. (2013). *National Coastal Population Report. Population trends from 1970 to 2020 (State of the Coast Report Series)*.
- NOAA. (2018). *Digital coast: Data access viewer*. Retrieved from <https://coast.noaa.gov/dataviewer/#/lidar/search/>
- Nyman, J. A., Walters, R. J., Delaune, R. D., & Patrick, W. H. (2006). Marsh vertical accretion via vegetative growth. *Estuarine, Coastal and Shelf Science*, *69*, 370–380. <https://doi.org/10.1016/j.ecss.2006.05.041>
- Paltan, H., Waliser, D., Lim, W. H., Guan, B., Yamazaki, D., Pant, R., & Dadson, S. (2017). Global floods and water availability driven by atmospheric rivers: Global hydrology and ARs. *Geophysical Research Letters*, *44*, 10387–10395. <https://doi.org/10.1002/2017GL074882>
- Payne (2021). Short-term effects of thin-layer sand placement on salt marsh grasses: A marsh organ field experiment. *Journal of Coastal Research*. <https://doi.org/10.2112/JCOASTRES-D-20-00072.1>
- Payne, A. E., Demory, M.-E., Leung, L. R., Ramos, A. M., Shields, C. A., Rutz, J. J., et al. (2020). Responses and impacts of atmospheric rivers to climate change. *Nature Reviews Earth & Environment*, *1*, 143–157. <https://doi.org/10.1038/s43017-020-0030-5>
- Peterson, G. W., & Turner, R. E. (1994). The value of salt marsh edge vs interior as a habitat for fish and decapod crustaceans in a Louisiana tidal marsh. *Estuaries*, *17*, 235. <https://doi.org/10.2307/1352573>
- Polade, S. D., Gershunov, A., Cayan, D. R., Dettinger, M. D., & Pierce, D. W. (2017). Precipitation in a warming world: Assessing projected hydro-climate changes in California and other Mediterranean climate regions. *Scientific Reports*, *7*, 10783. <https://doi.org/10.1038/s41598-017-11285-y>
- Poulos, S. E., & Collins, M. B. (2002). Fluvial sediment fluxes to the Mediterranean Sea: A quantitative approach and the influence of dams. *Geological Society, London, Special Publications*, *191*, 227–245. <https://doi.org/10.1144/GSL.SP.2002.191.01.16>
- Radić, V., Cannon, A. J., Menounos, B., & Gi, N. (2015). Future changes in autumn atmospheric river events in British Columbia, Canada, as projected by CMIP5 global climate models. *Journal of Geophysical Research: Atmospheres*, *120*, 9279–9302. <https://doi.org/10.1002/2015JD023279>
- Ralph, F. M., Rutz, J. J., Cordeira, J. M., Dettinger, M., Anderson, M., Reynolds, D., et al. (2019). A scale to characterize the strength and impacts of atmospheric rivers. *Bulletin of the American Meteorological Society*, *100*, 269–289. <https://doi.org/10.1175/BAMS-D-18-0023.1>
- Ralston, D. K., Warner, J. C., Geyer, W. R., & Wall, G. R. (2013). Sediment transport due to extreme events: The Hudson River estuary after tropical storms Irene and Lee: Ralston sediment transport due to extreme events. *Geophysical Research Letters*, *40*, 5451–5455. <https://doi.org/10.1002/2013GL057906>
- Ramos, A. M., Tomé, R., Trigo, R. M., Liberato, M. L. R., & Pinto, J. G. (2016). Projected changes in atmospheric rivers affecting Europe in CMIP5 models: Atmospheric rivers affecting EUROPE. *Geophysical Research Letters*, *43*, 9315–9323. <https://doi.org/10.1002/2016GL070634>
- Ramsey, E., Rangoonwala, A., Chi, Z., Jones, C. E., & Bannister, T. (2014). Marsh Dieback, loss, and recovery mapped with satellite optical, airborne polarimetric radar, and field data. *Remote Sensing of Environment*, *152*, 364–374. <https://doi.org/10.1016/j.rse.2014.07.002>
- Reed, D. J., Spencer, T., Murray, A. L., French, J. R., & Leonard, L. (1999). Marsh surface sediment deposition and the role of tidal creeks: Implications for created and managed coastal marshes. *Journal of Coastal Conservation*, *5*, 81–90. <https://doi.org/10.1007/BF02802742>
- Romme, W. H., Everham, E. H., Frelich, L. E., Moritz, M. A., & Sparks, R. E. (1998). Are large, infrequent disturbances qualitatively different from small, frequent disturbances? *Ecosystems*, *1*, 524–534. <https://doi.org/10.1007/s100219900048>
- Ruhl, C., Schoellhamer, D., & U.S. Geological Survey. (2004). Spatial and temporal variability of suspended-sediment concentrations in a Shallow Estuarine Environment. *San Francisco Estuary and Watershed Science*, *2*. <https://doi.org/10.15447/sfews.2004v2iss2art1>
- Schieder, N. W., Walters, D. C., & Kirwan, M. L. (2018). Massive upland to wetland conversion compensated for historical marsh loss in Chesapeake bay, USA. *Estuaries and Coasts*, *41*, 940–951. <https://doi.org/10.1007/s12237-017-0336-9>
- Schile, L. M., Callaway, J. C., Morris, J. T., Stralberg, D., Parker, V. T., & Kelly, M. (2014). Modeling tidal marsh distribution with sea-level rise: Evaluating the role of vegetation, sediment, and upland habitat in marsh resiliency. *PLoS One*, *9*, e88760. <https://doi.org/10.1371/journal.pone.0088760>

- Schuerch, M., Rapaglia, J., Liebetrau, V., Vafeidis, A., & Reise, K. (2012). Salt marsh accretion and storm tide variation: An example from a barrier island in the north sea. *Estuaries and Coasts*, *35*, 486–500. <https://doi.org/10.1007/s12237-011-9461-z>
- Schuerch, M., Vafeidis, A., Slawig, T., & Temmerman, S. (2013). Modeling the influence of changing storm patterns on the ability of a salt marsh to keep pace with sea level rise: Salt marsh accretion and storm activity. *Journal of Geophysical Research: Earth Surface*, *118*, 84–96. <https://doi.org/10.1029/2012JF002471>
- Sharpe, P. J., & Baldwin, A. H. (2012). Tidal marsh plant community response to sea-level rise: A mesocosm study. *Aquatic Botany*, *101*, 34–40. <https://doi.org/10.1016/j.aquabot.2012.03.015>
- Shields, C. A., & Kiehl, J. T. (2016). Atmospheric River landfall-latitude changes in future climate simulations: Future changes to AR landfall location. *Geophysical Research Letters*, *43*, 8775–8782. <https://doi.org/10.1002/2016GL070740>
- Smith, A. B. (2020). *2010–2019: A landmark decade of US. Billion-dollar weather and climate disasters*. National Oceanic and Atmospheric Administration.
- Smith, K. R., Barthman-Thompson, L., Gould, W. R., & Mabry, K. E. (2014). Effects of natural and anthropogenic change on habitat use and movement of endangered salt marsh harvest mice. *PLoS One*, *9*, e108739. <https://doi.org/10.1371/journal.pone.0108739>
- Smith, J. E., Bentley, S. J., Snedden, G. A., & White, C. (2015). What role do hurricanes play in sediment delivery to subsiding river deltas? *Scientific Reports*, *5*, 17582. <https://doi.org/10.1038/srep17582>
- Stagg, C. L., Osland, M. J., Moon, J. A., Feher, L. C., Laurenzano, C., Lane, T. C., et al. (2021). Extreme precipitation and flooding contribute to sudden vegetation dieback in a coastal Salt Marsh. *Plants*, *10*, 1841. <https://doi.org/10.3390/plants10091841>
- Stralberg, D., Brennan, M., Callaway, J. C., Wood, J. K., Schile, L. M., Jongsomjit, D., et al. (2011). Evaluating tidal marsh sustainability in the face of sea-level rise: A hybrid modeling approach applied to San Francisco bay. *PLoS One*, *6*, e27388. <https://doi.org/10.1371/journal.pone.0027388>
- Swanson, K. M., Drexler, J. Z., Schoellhamer, D. H., Thorne, K. M., Casazza, M. L., Overton, C. T., et al. (2014). Wetland accretion rate model of ecosystem resilience (WARMER) and its application to habitat sustainability for endangered species in the San Francisco estuary. *Estuaries and Coasts*, *37*, 476–492. <https://doi.org/10.1007/s12237-013-9694-0>
- Taylor, M. (2017). Managing floods in California. *Legislative Analyst's Office Report*.
- Temmerman, S., Govers, G., Wartel, S., & Meire, P. (2003). Spatial and temporal factors controlling short-term sedimentation in a salt and freshwater tidal marsh, Scheldt estuary, Belgium, SW Netherlands. *Earth Surface Processes and Landforms*, *28*, 739–755. <https://doi.org/10.1002/esp.495>
- Temmerman, S., Meire, P., Bouma, T. J., Herman, P. M. J., Ysebaert, T., & De Vriend, H. J. (2013). Ecosystem-based coastal defence in the face of global change. *Nature*, *504*, 79–83. <https://doi.org/10.1038/nature12859>
- Thorne, K., MacDonald, G., Guntenspergen, G., Ambrose, R., Buffington, K., Dugger, B., et al. (2018). U.S. Pacific coastal wetland resilience and vulnerability to sea-level rise. *Science Advances*, *4*, eaao3270. <https://doi.org/10.1126/sciadv.aao3270>
- Thorne, K. M., Freeman, C. M., Buffington, K. J., & Janousek, C. N. (2022). *Wetland elevation change, accretion, and water level data for San Francisco Bay-Delta*. U.S. Geological Survey data release. <https://doi.org/10.5066/P95UFMIS>
- Thorne, K. M., Spragens, K. A., Buffington, K. J., Rosencranz, J. A., & Takekawa, J. (2019). Flooding regimes increase avian predation on wild-life prey in tidal marsh ecosystems. *Ecology and Evolution*, *9*, 1083–1094. <https://doi.org/10.1002/ece3.4792>
- Turner, M. G. (2010). Disturbance and landscape dynamics in a changing world. *Ecology*, *91*, 2833–2849. <https://doi.org/10.1890/10-0097.1>
- Turner, R. E., Baustian, J. J., Swenson, E. M., & Spicer, J. S. (2006). Wetland sedimentation from hurricanes Katrina and Rita. *Science*, *314*, 449–452. <https://doi.org/10.1126/science.1129116>
- United States Census Bureau. (2019). *2014–2018 American Community Survey (ACS) 5-year estimates*. United States government. <https://data.census.gov/cedsci/>
- Van DePol, M., Ens, B. J., Heg, D., Brouwer, L., Krol, J., Maier, M., et al. (2010). Do changes in the frequency, magnitude and timing of extreme climatic events threaten the population viability of coastal birds?: Climate change and nest flooding risk. *Journal of Applied Ecology*, *47*, 720–730. <https://doi.org/10.1111/j.1365-2664.2010.01842.x>
- van derWegen, M., Roelvink, J. A., & Jaffe, B. E. (2019). Morphodynamic resilience of intertidal mudflats on a seasonal time scale. *Journal of Geophysical Research: Oceans*, *124*, 8290–8308. <https://doi.org/10.1029/2019JC015492>
- Vázquez-González, C., Moreno-Casasola, P., Peralta Peláez, L. A., Monroy, R., & Espejel, I. (2019). The value of coastal wetland flood prevention lost to urbanization on the coastal plain of the Gulf of Mexico: An analysis of flood damage by hurricane impacts. *International Journal of Disaster Risk Reduction*, *37*, 101180. <https://doi.org/10.1016/j.ijdrr.2019.101180>
- Wahl, T., Jain, S., Bender, J., Meyers, S. D., & Luther, M. E. (2015). Increasing risk of compound flooding from storm surge and rainfall for major US cities. *Nature Climate Change*, *5*, 1093–1097. <https://doi.org/10.1038/nclimate2736>
- Waliser, D., & Guan, B. (2017). Extreme winds and precipitation during landfall of atmospheric rivers. *Nature Geoscience*, *10*, 179–183. <https://doi.org/10.1038/ngeo2894>
- Wang, S., Anichowski, A., Tippet, M. K., & Sobel, A. H. (2017). Seasonal noise versus subseasonal signal: Forecasts of California precipitation during the unusual winters of 2015–2016 and 2016–2017: S2S forecast of CA precipitation. *Geophysical Research Letters*, *44*, 9513–9520. <https://doi.org/10.1002/2017GL075052>
- Warren, R. S., & Niering, W. A. (1993). Vegetation change on a northeast tidal marsh: Interaction of sea-level rise and marsh accretion. *Ecology*, *74*, 96–103. <https://doi.org/10.2307/1939504>
- Webb, E. L., Friess, D. A., Krauss, K. W., Cahoon, D. R., Guntenspergen, G. R., & Phelps, J. (2013). A global standard for monitoring coastal wetland vulnerability to accelerated sea-level rise. *Nature Climate Change*, *3*, 458–465. <https://doi.org/10.1038/nclimate1756>
- Wen, Y., Behrang, A., Chen, H., & Lambriksen, B. (2018). How well were the early 2017 California Atmospheric River precipitation events captured by satellite products and ground-based radars? *Quarterly Journal of the Royal Meteorological Society*, *144*, 344–359. <https://doi.org/10.1002/qj.3253>
- Wright, S., & Schoellhamer, D. H. (2004). Trends in the sediment yield of the Sacramento River, California, 1957–2001. *San Francisco Estuary Watershed Science* (Vol. 2). California: eScholarship University of California. <https://doi.org/10.15447/sfews.2004v2iss2art2>
- Yang, S. L. (2005). Impact of dams on Yangtze River sediment supply to the sea and delta intertidal wetland response. *Journal of Geophysical Research*, *110*, F03006. <https://doi.org/10.1029/2004JF000271>
- Yeates, A. G., Grace, J. B., Olker, J. H., Guntenspergen, G. R., Cahoon, D. R., Adamowicz, S., et al. (2020). Hurricane sandy effects on coastal marsh elevation change. *Estuaries and Coasts*, *43*, 1640–1657. <https://doi.org/10.1007/s12237-020-00758-5>
- Yellen, B., Woodruff, J., Ladlow, C., Ralston, D. K., Fernald, S., & Lau, W. (2021). Rapid tidal marsh development in anthropogenic backwaters. *Earth Surface Processes and Landforms*, *46*, 554–572. <https://doi.org/10.1002/esp.5045>
- Zhu, Y., & Newell, R. (1998). A proposed algorithm for moisture fluxes from atmospheric rivers. *Monthly Weather Review*, *126*, 725–735. [https://doi.org/10.1175/1520-0493\(1998\)126<0725:apafmf>2.0.co;2](https://doi.org/10.1175/1520-0493(1998)126<0725:apafmf>2.0.co;2)